Numerical Simulation of Acoustic Characteristics of Iced Rotors based on the HMB Method

Xi Chen[1,2], Qijun Zhao[1], George N. Barakos[2], Alexander Kusyumov[3]

1 Nanjing University of Aeronautics and Astronautics, Nanjing, PR China
[2] School of Engineering, University of Glasgow, Scotland, U.K.
[3]KNRTU-KAI n.a. A. Tupolev, Kazan, Russia

Background and Motivation

Ice accretion for helicopter, especially on rotors, can be **a serious threat to flight safety**.

When helicopters fly in icing conditions, the ice accretion may occur on the rotor blades, and their designed aerodynamic shape may be modified and degraded. This resulted in serious accidents[1].

- A large increase in rotor required power
- A large decrease in rotor lift
- A serious threat to flight safety

[1]Rosen, K. M., Potash, M. L., "40 years of helicopter ice protection experience at Sikorsky aircraft", AIAA paper 1981-0407, 1987.

Development of Numerical Simulation Methods for Aircraft Icing

Year	Main Research Topics
1940's	Taylor and Langmuir respectively **built the supercool water droplet movement equations** according to Newton's second law, and Langmuir also established a method to calculated droplet trajectories based on the air flowfield information.
1953	Messinger made an outstanding contribution for icing prediction. He used a quasi-steady assumption for icing process to establish an icing model, and it is known as **Messinger's icing model** today.
1982	MacArthur **established a numerical simulation method for ice accretion**, which is divided into three steps: flowfield solution, water droplet trajectory calculation and icing model.
recent years	several codes for simulating ice accretion on aircrafts are also developed successfully, such as: **LEWICE, ONERA, FENSAP-ICE, etc.**

Taylor, G. I., "Notes on Possible Equipment and Technique for Experiments on Icing on Aircraft. British Aeronautical Research Council", R&G, No. 2024, Jan. 1940.
Langmuir, I., Blodgett, K., "A Mathematical Investigation of Water Droplet Trajectories," Army Air Force Technical Report No.5418, Dec. 1946.
Messinger, B. L., "Equilibrium Temperatuer of an Unheated Icing Surface as a Function of Airspeed", *Journal of the Aeronautical Sciences*, Vol. 20, No. 1, 1953, pp. 29-42.
Macarthur, C. D., "Numerical Simulation of Airfoil Ice Accretion", AIAA 1983-0112, 1983
Wright, W., "Further Refinement of the LEWICE SLD Model," AIAA paper 2006-0464, 2006.
Hedde, T., and Guffond, D., "ONERA Three-Dimensional Icing Model," *AIAA Journal*, Vol. 33, No.6, 1995, pp. 1038-1044.
Nilamdeen, S., Habashi, W. G., Aubé, M. S., and Baruzzi, G. S., "FENSAP-ICE: Modeling of Water Droplets and Ice Crystals," AIAA paper 2009-4128, 2009.

Further Development of Numerical Icing Models

Year	Main Research Topics
1998	Tsao investigated the formation of surface roughness on the surface of airfoils **through the stability analysis of air/liquid, water/ice, and substrate interfaces**.
2002	Blackmore, introduced an icing model that describes **spongy ice formation** in atmospheric icing, and a dendritic-growth layer is assumed to relate the microscopic ice growth with the macroscopic mass/energy conservation.
2004	Fortin developed a new analytical model for **the calculation of roughness heights** and a new geometric ice addition model based on bisection of the angle between adjacent panels.
2014	Kong developed **an aircraft supercooled icing model**, in which **the influences of the flow velocity on ice growth are taken into account**.

Tsao, J. C., Rothmayer, A. P., "A Mechanism for Ice Roughness Formation on an Airfoil Leading Edge, Contributing to Glaze Ice Accretion," AIAA Paper 1998-0485, Jan. 1998.

Fortin, G., Ilinca, A., Laforte, J.-L., Brandi, V., "New Roughness Computation Method and Geometric Accretion Model for Airfoil Icing," *Journal of Aircraft*, Vol. 41, No. 1, 2004, pp. 119-127.

Blackmore, R. Z., Makkonen, L., Lozowski, E. P., "A New Model of Spongy Icing from First Principles," *Journal of Geophysical Research*, Vol. 107, No. D21, 2002, pp. 9-1–9-15.

Kong, W., Liu, H., "Development and Theoretical Analysis of an Aircraft Supercooled Icing Model," *Journal of Aircraft*, Vol. 51, No.3, 2014, pp. 975-986.

Development of Numerical Simulation Methods for Aircraft Icing

Year	Rotors in Hover
2010	Kinzel developed a finite volume approach to modeling ice accretion on rotors, and the droplet trajectory is determined **using a 3-D Eulerian approach**.
2012	Narducci developed an analysis method to evaluate the ice accumulation for a helicopter flying through an icing cloud **based on blade sections**.
2012	Zhong investigated the numerical simulation for ice accretion on **UH-60 and CH-47 helicopter rotor** using **a simple 2-D section method**.
2016	Zhao proposed a numerical method for ice accretion on rotor in hover, and takes the influence of centrifugal force into account. Through the comparisons results in his calculation, **the centrifugal force really affects the movement of unfrozen water film on blade surface**.
2017	Wang also developed a similar method to predicting ice accretion on rotor in hovering flight, and he also found that **the effect of centrifugal force is important for ice accretion on rotors**.

Narducci, R., Kreeger, R., "Analysis of a Hovering Rotor in Icing Conditions," NASA TM-217126, 2012.

Zhong, G., Cao, Y., ZHAO, M., "Numerical Simulation of Ice Accretion on Helicopter Rotor, Journal of Beijing University of Aeronautics And Astronautics," Vol 38, No. 3, 2012, pp.101-111.

Kinzel, M. P., Sarofeen, C. M., Noack, R. W., "A finite-volume approach to modeling ice accretion", AIAA Paper 2010-4230, 2010.

G. Q., Zhao, Q. J., Chen, X., "New 3-D ice accretion method of hovering rotor including effects of centrifugal force," Aerospace Science and Technology, Vol. 48, 2016, pp. 122-130.

Wang, Z. Z., Zhu, C. L., "Study of the Effect of Centrifugal Force on Rotor Blade Icing Process," *International Journal of Aerospace Engineering*, Volume 2017 (2017), Article ID 8695170, 9 pages, doi:10.1155/2017/8695170

Year	Rotors in Forward Flight
2010	Rajmohan developed **a quasi-steady numerical method** for ice accretion on helicopter rotors in forward flight using the LEWICE3D.
2010	Bain used the same approach to predict the ice accretion and ice shedding on rotors.
2011	Aliaga developed **a new code by coupling in time the dilute two-phase flow (air and water droplets flow) with ice accretion**, and the unsteady model is shown to open the door for a unified approach to icing on jet engines, on fixed wings and on helicopters with rotors/fuselage systems.
2012	Narducci developed **a high-fidelity icing analysis method**, and do some simulation for a model-scale rotor in forward flight.
2012	Matsuura did some calculation of ice accretion on rotor blade of axial blower, and he found **ice is not formed in the very vicinity of the hub**.
2016	Son predicted the ice shape on the helicopter fuselage **considering rotor-wake effects**, and **the droplet collection amount and total ice amount are less** when rotor wake is considering.

Son, C., "Ice Accretion on Helicopter Fuselage Considering Rotor-Wake Effects", Journal of Aircraft, (2016), accessed August 30, 2016. doi:10.2514/1.C033830.
Rajmohan, N., "Icing Studies for the UH-60A Rotor in Forward Flight," Proceedings of the 2010 AHS Aeromechanics Specialists' Conference, American Helicopter Society, San Francisco, CA, Jan 20-22, 2010, pp. 261-276.
Bain, J.,"Prediction of Rotor Blade Ice Shedding Using Empirical Methods," AIAA paper 2010-7985, 2010.
Narducci, R., "Application of a High-Fidelity Icing Analysis Method to a Model-Scale Rotor in Forward Flight", NASA TM-217122.
Matsuura, T., "Numerical simulation of ice accretion phenomena on rotor blade of axial blower," *Journal of Thermal Science*, Vol. 21, No. 4, 322-326, 2012.
Aliaga, C. N., "Fensap-ice-unsteady: unified in-flight icing simulation methodology for aircraft, rotorcraft, and jet engines", *Journal of Aircraft*, Vol. 48, No.1, January-february, 2011.

Ice Detection Methods

Usually, the icing conditions ahead flight route are estimated **from radars or other environmental sensors**, hence flight paths are changed, or, if it exists, anti-icing/de-icing systems are used.

Icing detection sensors

THERMAL
- **Pulse current method**
- **Temperature differential method**
- **Heat flux method**
- **……**

OPTICAL
- **Visual-Manual method**
- **Video camera method**
- **Infrared sensing method**
- **……**

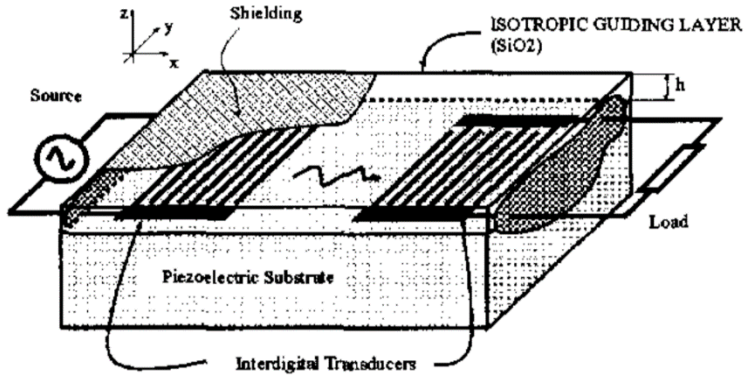

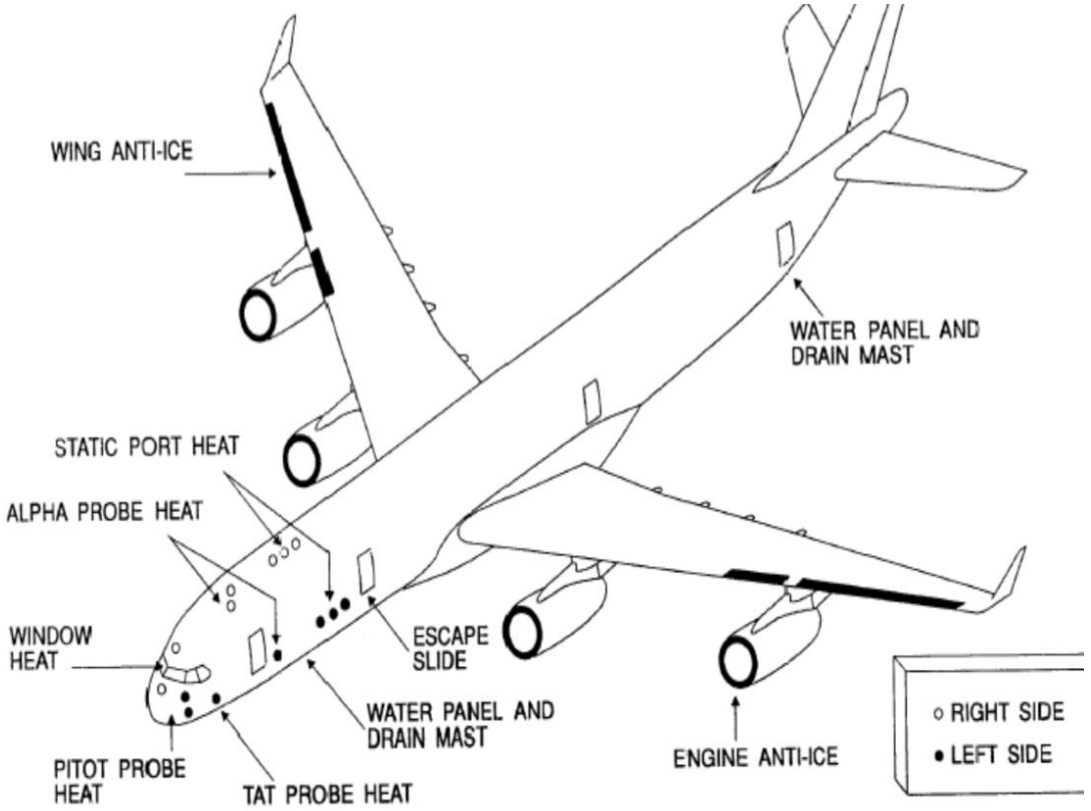

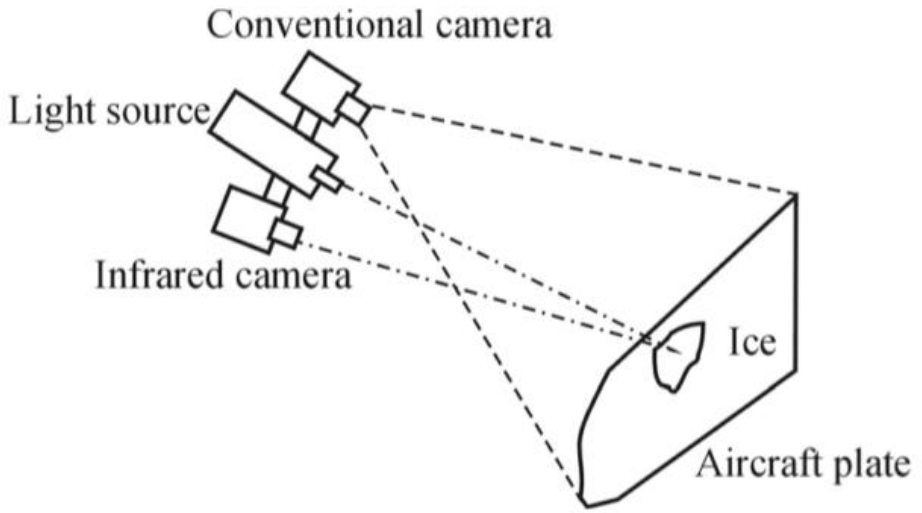

Compared to its fixed-wing counterpart, helicopter rotor ice accretion is **not well understood** due to complexities in the 3-D environment with inherent unsteady and rotational flow. So, it is **difficult to predict the rotor icing phenomenon** through the analysis of the temperature and other meteorological parameters.

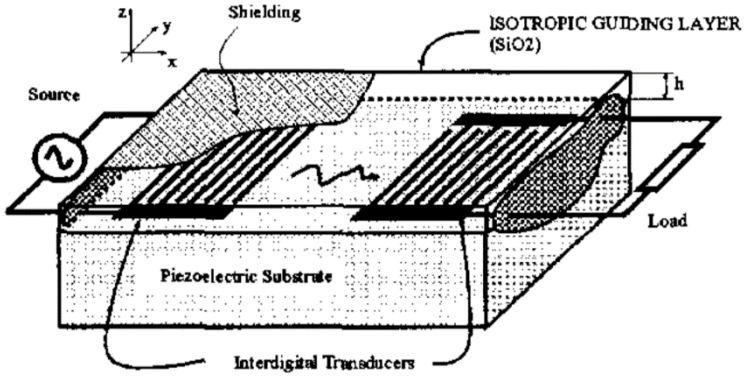

Temperature Sensor

The interior space of blade is very **limited**, some typical sensors might be difficult to amount, such as temperature sensors.

Due to **the complex motion of rotor**, such as rotor flapping, regular ice detection methods like infrared detectors are also **difficult** to implement.

Infrared detector system

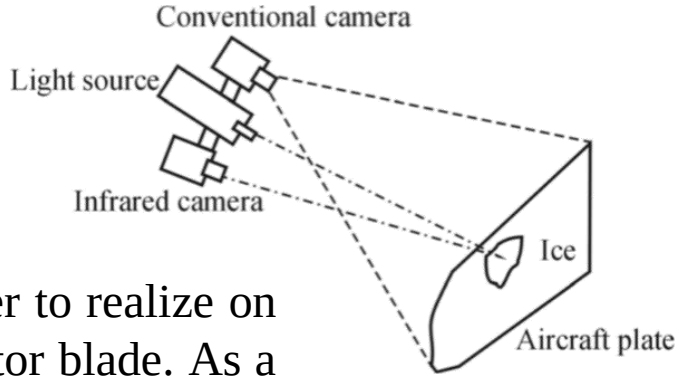

Microphone do not have to be mounted on the rotor, and are easier to realize on the helicopter fuselage, with no need to change the structure of rotor blade. As a result, sound **may be able to provide an icing detection method.**

Possible approach to icing detection

Cheng, B. F., Han, Y. Q., Brentner, K. S., and et al. “Rotor Broadband Noise due to Surface Roughness during Ice Accretion,” AIAA paper 2016-1270, 2016

Year	Main Research Contents
2016	Based on experiment and numerical simulation method, Cheng found the change of the flow behavior and blade shape by ice accretion is likely to affect the helicopter main rotor noise and it shows that **rotor noise can be used to detect the formation of accreted ice** at the early stage of ice accretion.

Objectives of this Work

- **To simulate the influence of ice on the acoustic characteristics of rotors**
- **To find best microphone positions for detecting icing (i.e. a distance between the rotor plane and microphones to detect icing)**
- **To estimate possibility of icing positions localization using the microphones array**

Considered Calculation Cases

Calculation Case		Content	Equations	Simulation tools
I	**2-D airfoil**	A. Validation of clean and iced airfoils	RANS	HMB solver
II	**Rotor in hover** (CT rotor)	A. Validation of clean rotor B. The influence of ice on aerodynamic characteristic C. The influence of ice on acoustic characteristic of the rotor D. The influence of ice amount on acoustic characteristic E. The influence of icing position along the span-wise direction on acoustic characteristic	RANS, FW-H	HMB solver, HFWH solver
III	**Rotor in forward flight** (UH-60A rotor)	A. Validation of clean rotor B. The influence of ice on aerodynamic characteristic C. The influence of ice on acoustic characteristic of rotor	URANS, FW-H	HMB solver, HFWH solver

Calculation Case I:
AG40 Effort – 2009

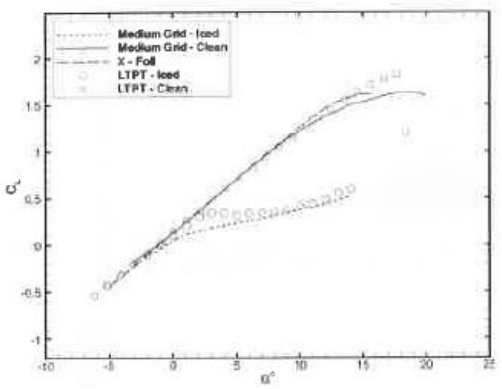

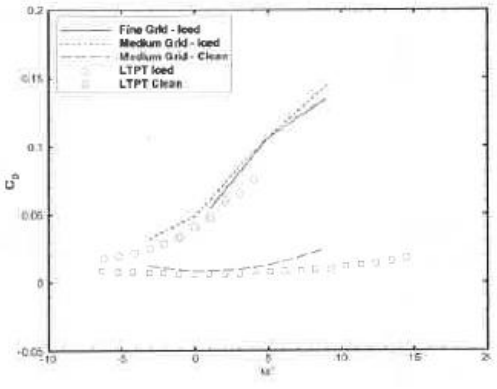

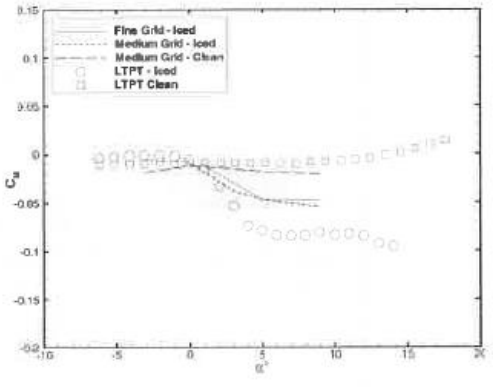

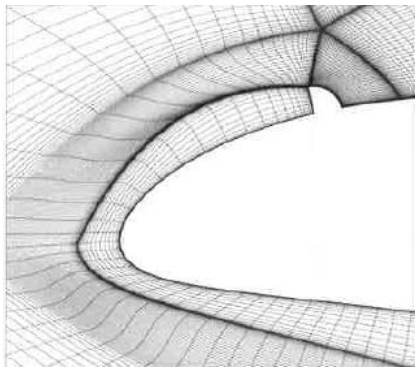

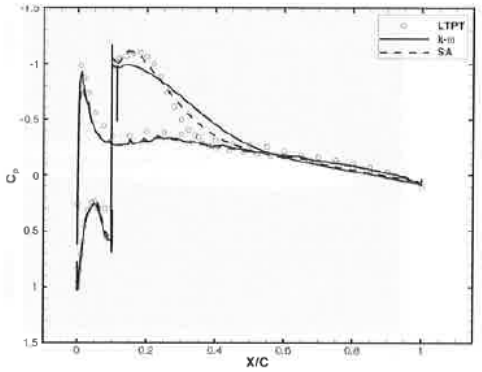

(a) α = 0°

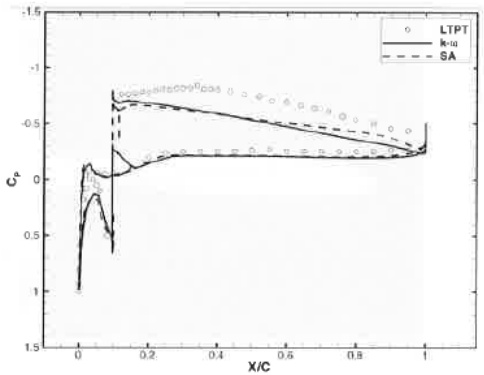

(b) α = 5°

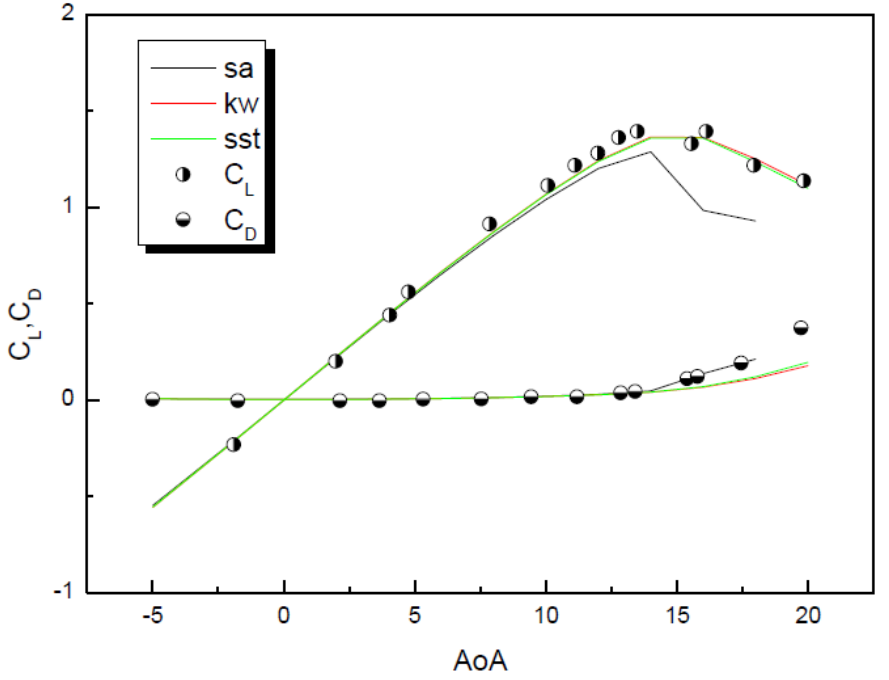

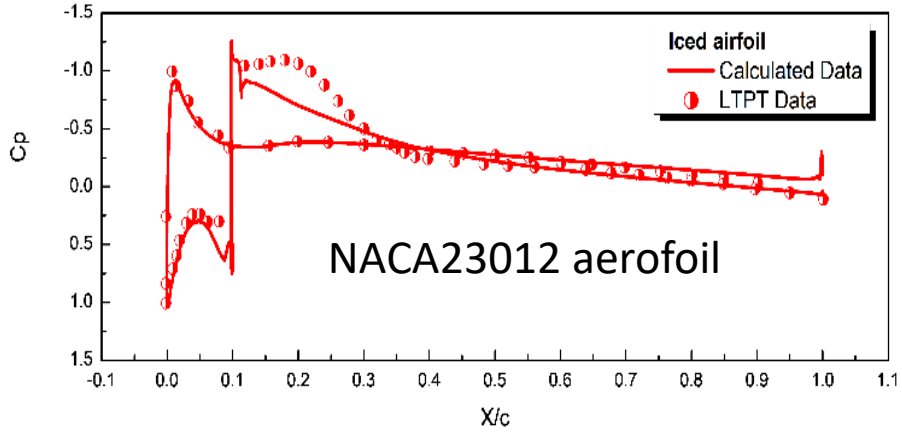

NASA Langley, Low Turbulence Pressure Tunnel – LTPT
Data provided by Univ. of Illinois Urbana-Champaign - UIUC

Calculation Case I: ICED NACA23012 AIRFOIL CALCULATION

The experimental data for an iced NACA23012 airfoil, obtained at the NASA Langley Low Turbulence Pressure Tunnel (LTPT) is selected to validate the accuracy of the employed numerical method.

The LTPT measurements were at a Mach number of 0.208 and at a Reynolds number of approximately 2×10^6.

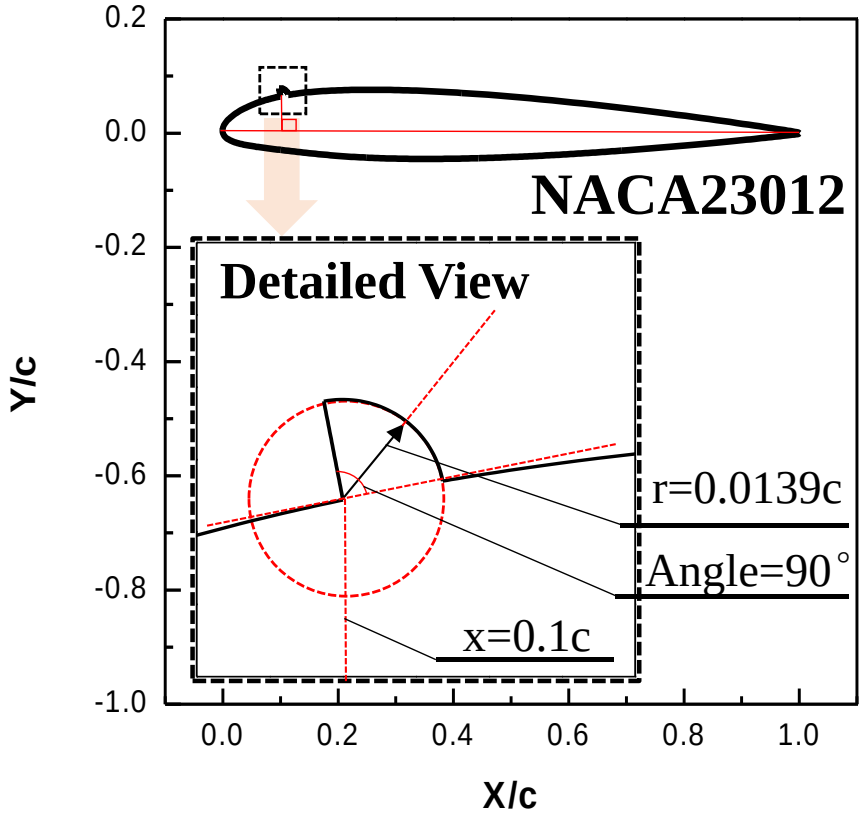

Detailed view of the ice shape and the modified NACA23012 section.

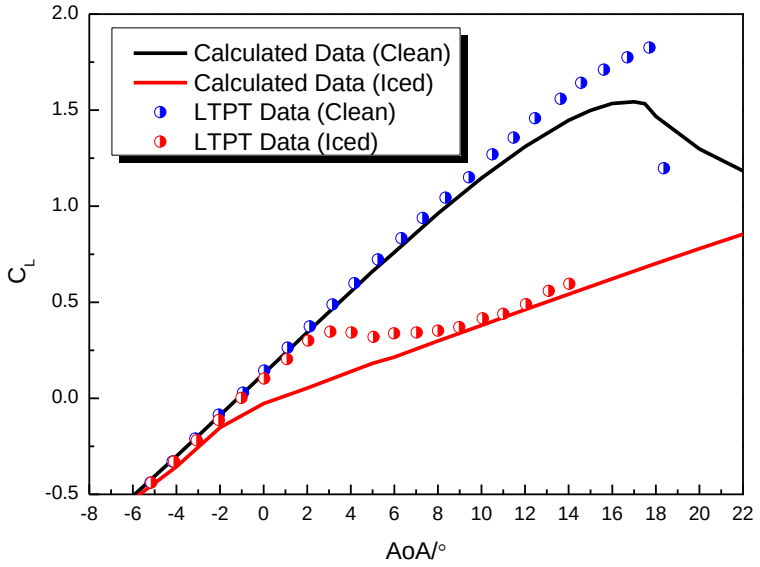

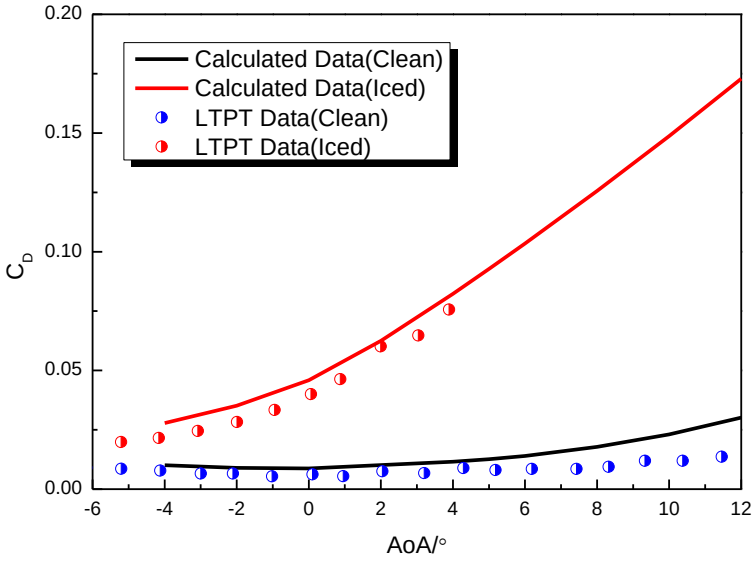

Aerodynamic characteristics of NACA 23012 airfoil with and without ice.

Comparisons of CL and CD with experimental data show fair agreement. When ice forms on the airfoil, the lift force decreases, and the drag force increases.

CC II: ACOUSTIC CHARACTERISTICS OF ROTORS IN HOVER WITH AND WITHOUT ICE

The CT rotor has two rectangular blades with a conventional NACA 0012 airfoil. For the iced rotor, the icing positions were from 0.6R to 0.9R along the blade.

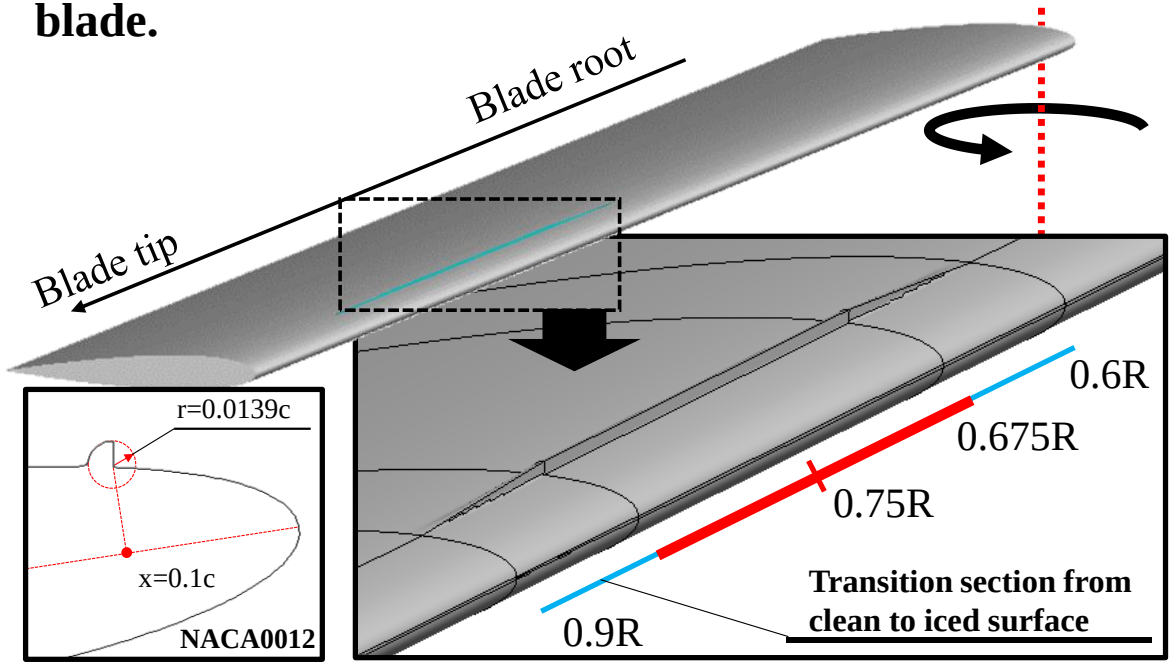

Icing position on the C-T rotor and sectional ice shape

Clean and iced cases for this rotor at Mtip=0.794 and at Re=3.48×10^6 and at a collective pitch of 8° were calculated.

Aerodynamic characteristics	C_T	C_Q	FM
Clean Rotor	1.10×10^{-2}	1.17×10^{-3}	0.492
Iced Rotor	0.61×10^{-2}	1.54×10^{-3}	0.156
Variation	-44.1%	+31.5%	-68.2%

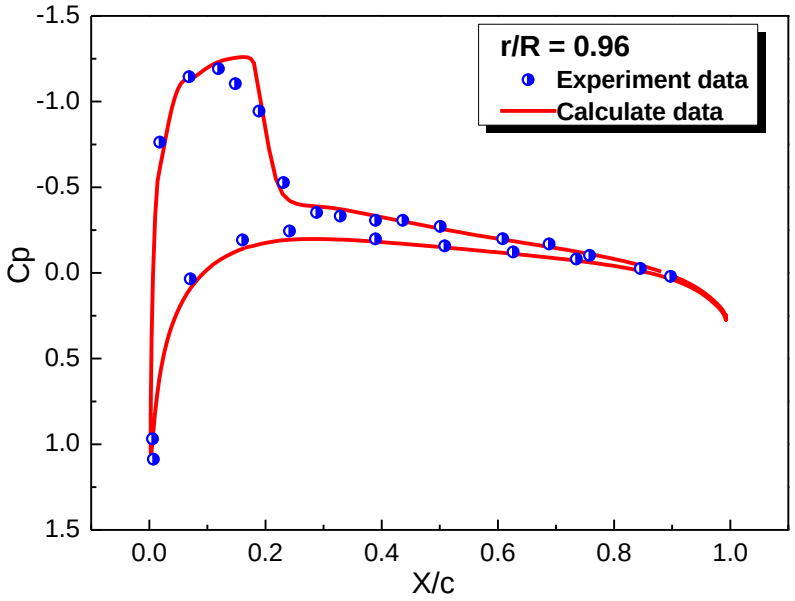

Comparison of the sectional pressure distribution of clean C-T rotor with experiment data.

5M cells for hover (single blade) with the Chimera method

SST-kw

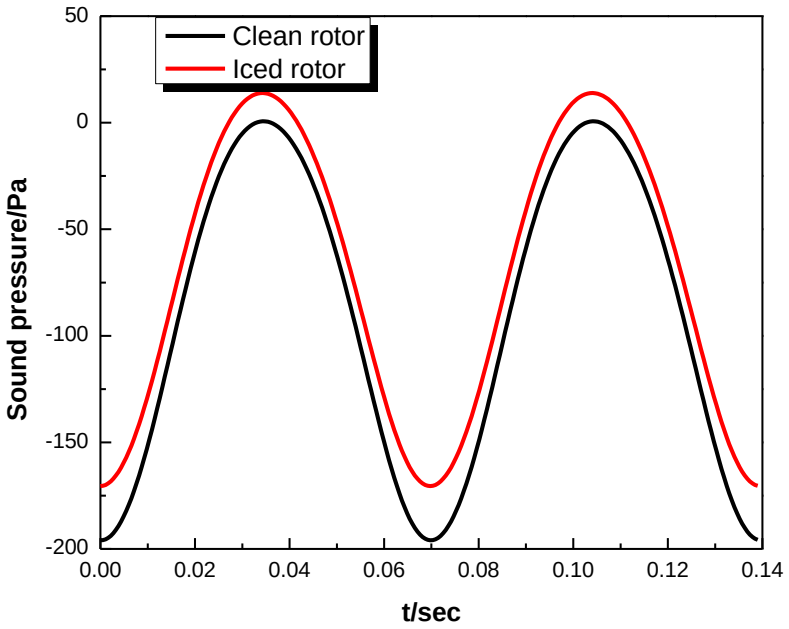

(a) Loading noise

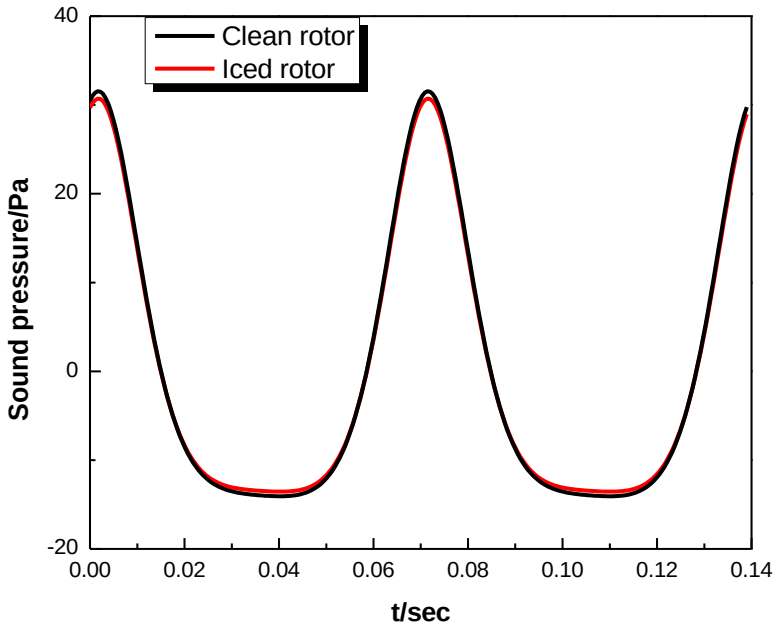

(b) Thickness noise

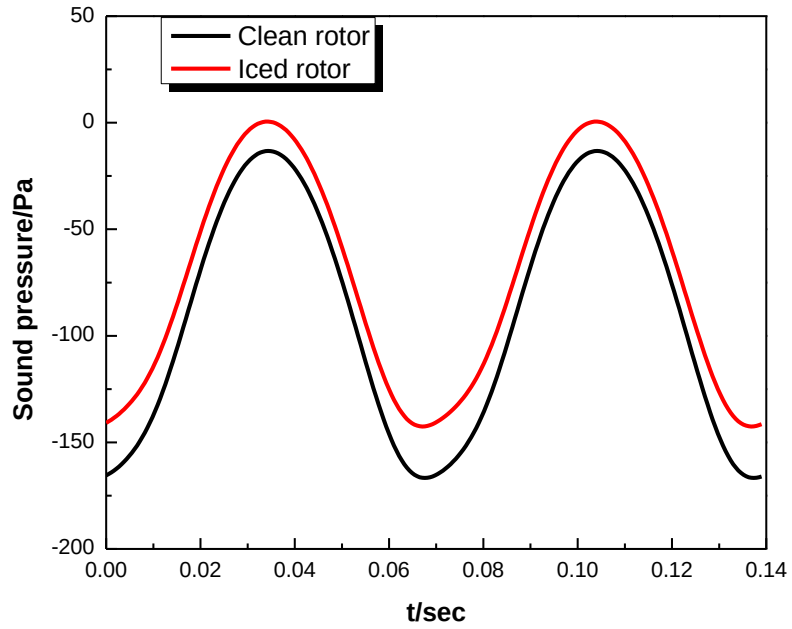

(c) Total noise

Sound pressure time histories at a typical monitoring position (r=0.25R, z=-0.25R)

The main difference of the effective sound pressure comes from loading noise, while the thickness noise is almost unchanged. (FW-H solution)

Considering the installation of acoustic monitors on the fuselage, all monitors are below the rotating plate, and their location is defined by the coordinates (r, z).

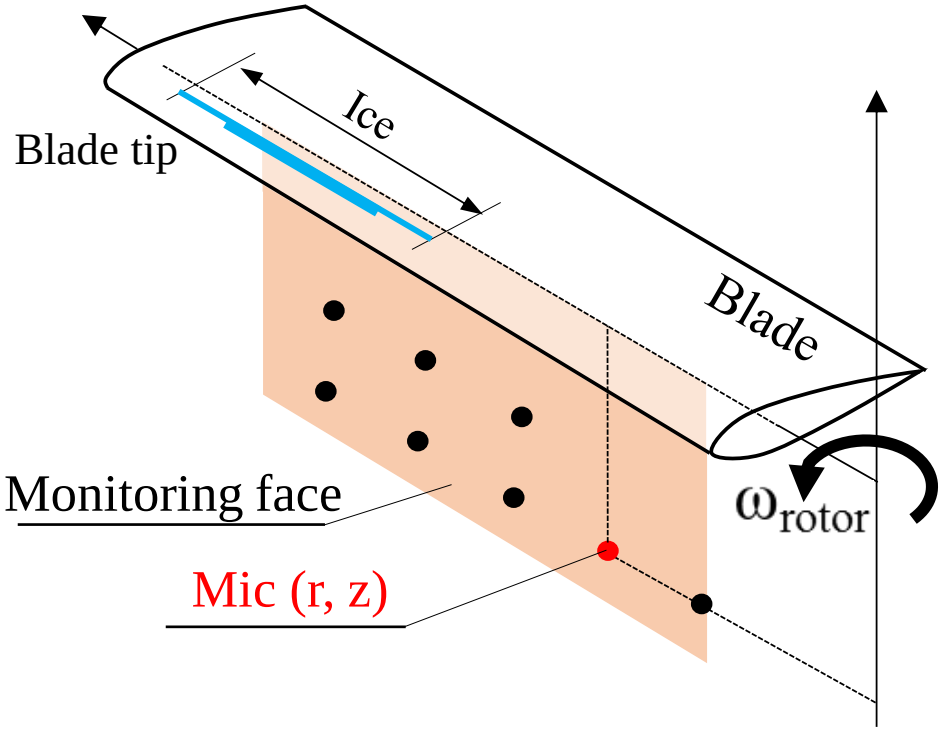

Positions of acoustics monitors relative to the blade.

On the z=-0.5R plane, the effective sound pressure of the iced rotor decreases compared with the clean rotor. This is because the lift force of the iced rotor drops.
On the z=-0.25R plane, the effective sound pressure first increases and then decreases.

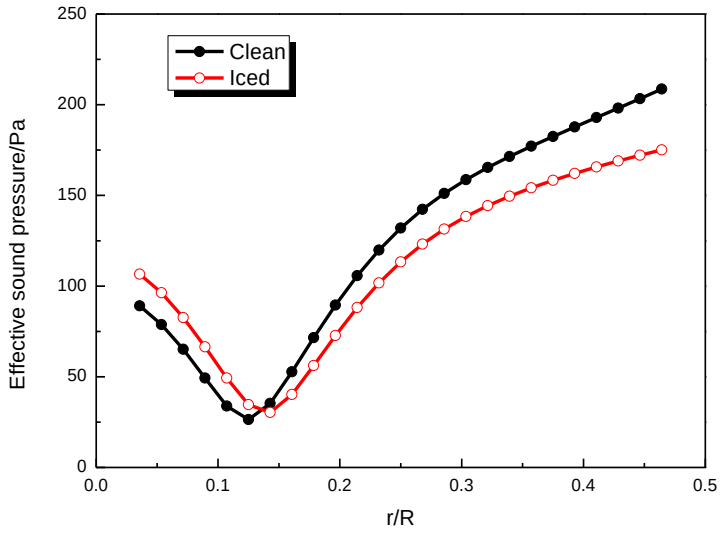

(a) z=-0.25R

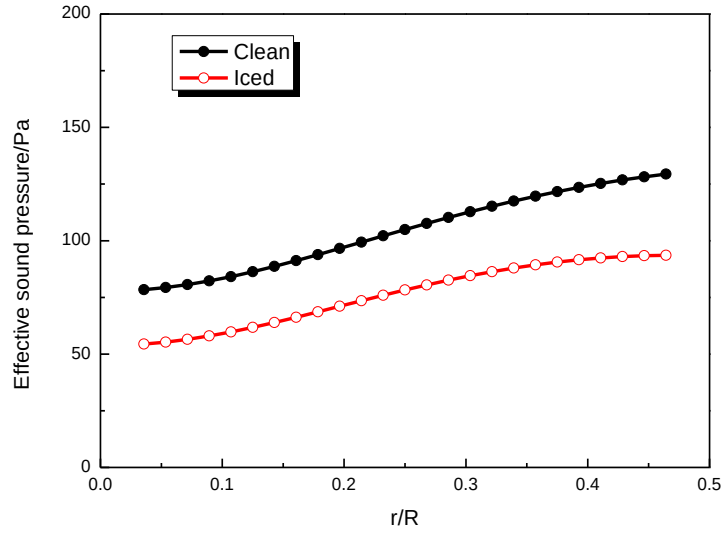

(b) z=-0.5R

Effective sound pressure at different monitor positions for clean and iced rotors

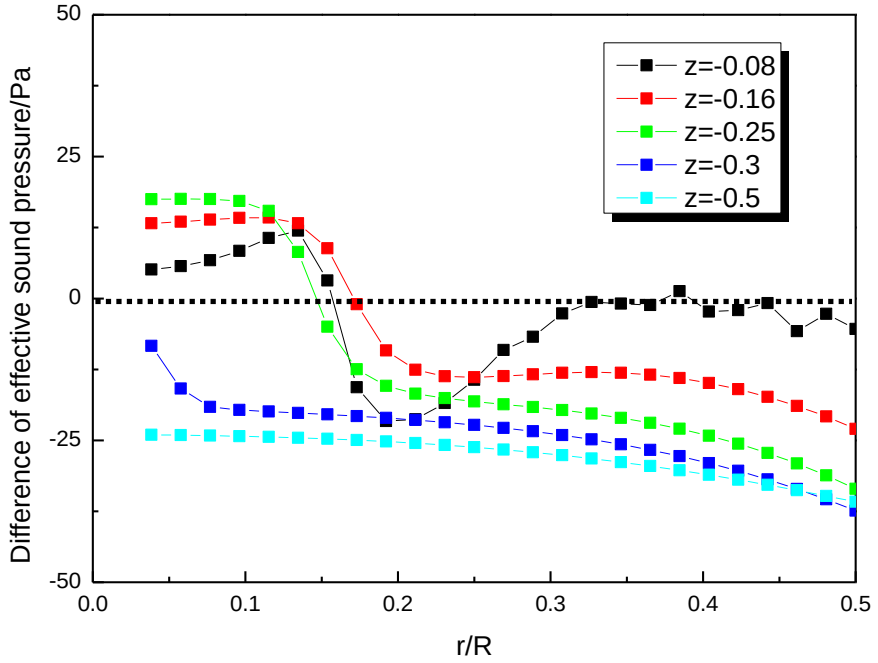

Difference of the effective sound pressure between clean and iced rotors at different z planes

When the monitor is far away from the rotor plane, the effective sound pressures of all monitors decrease.
When monitors are close to the rotor plane, the effective sound pressure changes significantly in the radial direction. It increases in places, and decreases in others.

The variation of sound pressure is evident in this case, indicating that ice can be detected based on the variation of the blade acoustic characteristics.

$$\Delta P_{ic} = P_i - P_c$$

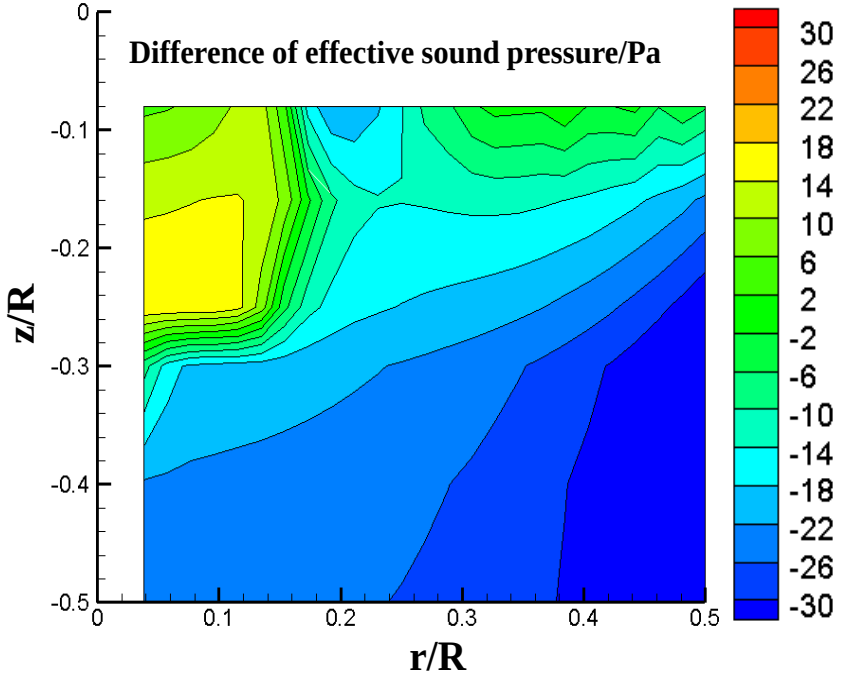

Difference of the effective sound pressure between clean and iced rotors

Acoustic characteristics of iced rotor with different ice amount.

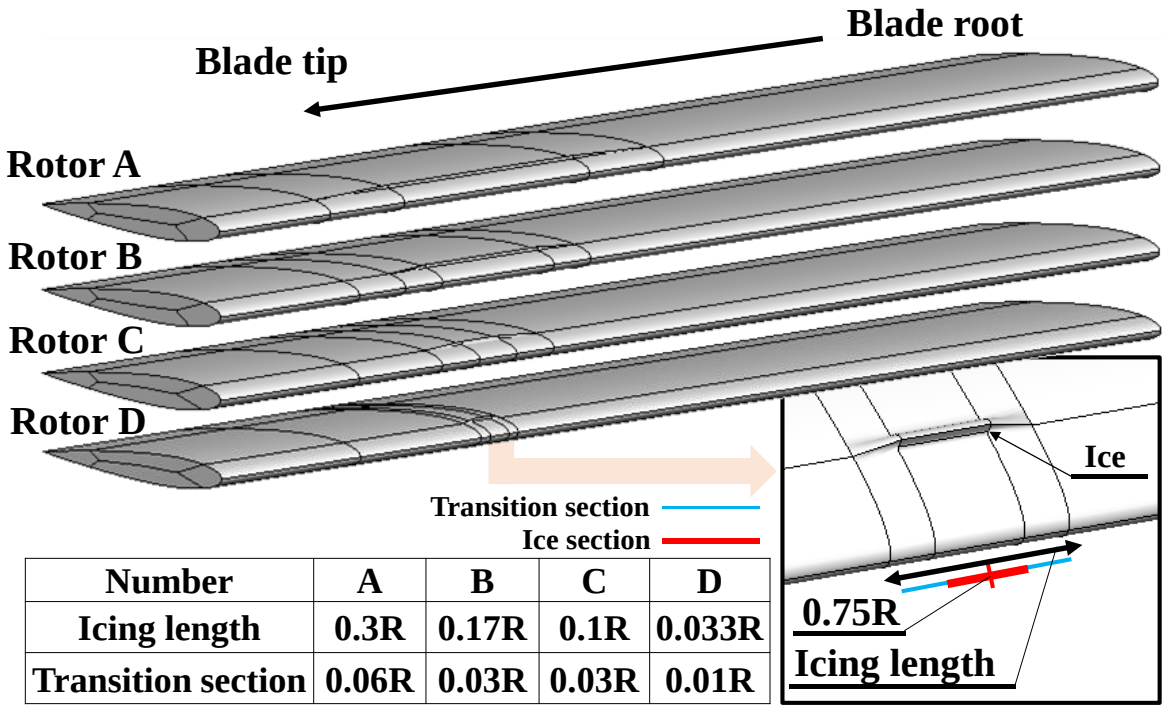

Number	A	B	C	D
Icing length	0.3R	0.17R	0.1R	0.033R
Transition section	0.06R	0.03R	0.03R	0.01R

Aerodynamic characteristics	C_T	C_Q	FM	Variation of FM
Clean	1.10×10^{-2}	1.17×10^{-3}	0.492	
Rotor A	0.61×10^{-2}	1.54×10^{-3}	0.156	-68.2%
Rotor B	0.91×10^{-2}	1.36×10^{-3}	0.318	-35.4%
Rotor C	1.04×10^{-2}	1.29×10^{-3}	0.409	-16.8%
Rotor D	1.06×10^{-2}	1.21×10^{-3}	0.454	-7.69%

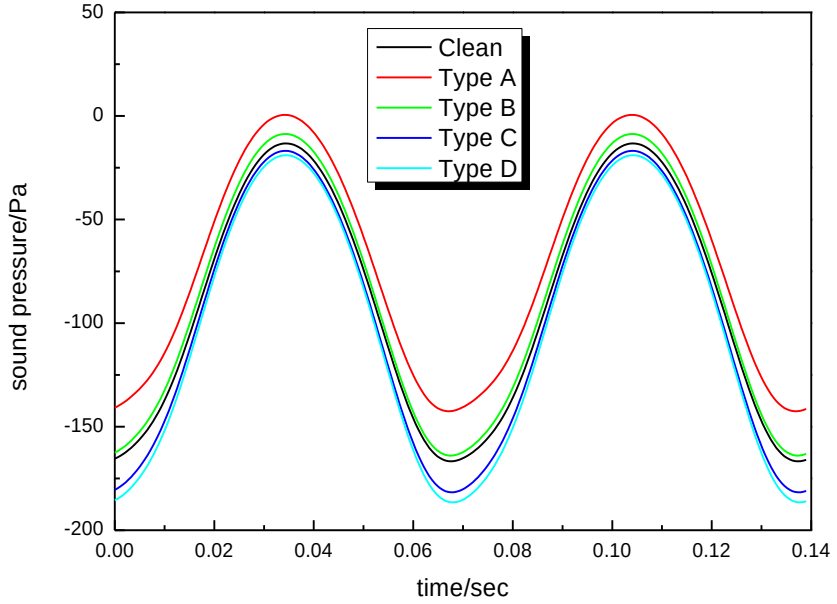

r=0.25R, z=-0.25R

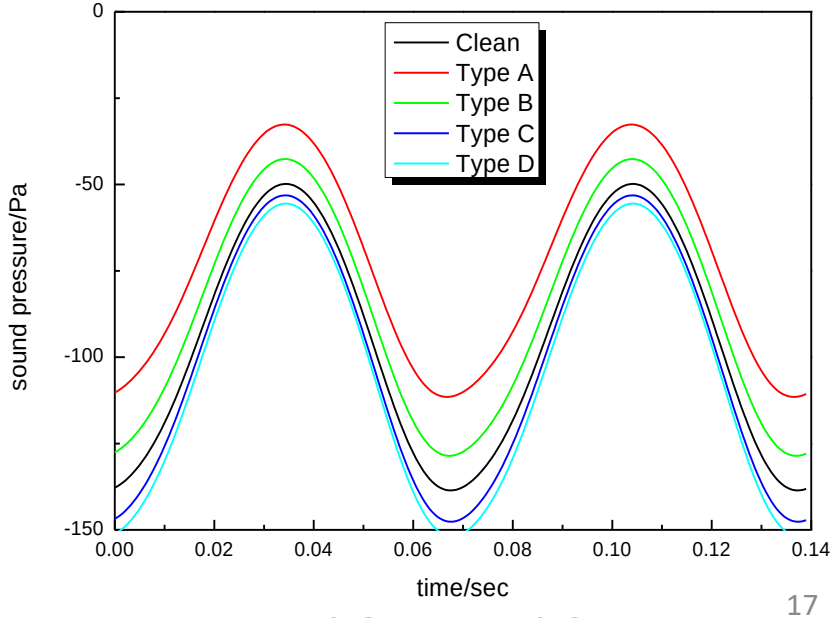

r=0.25R, z=-0.3R

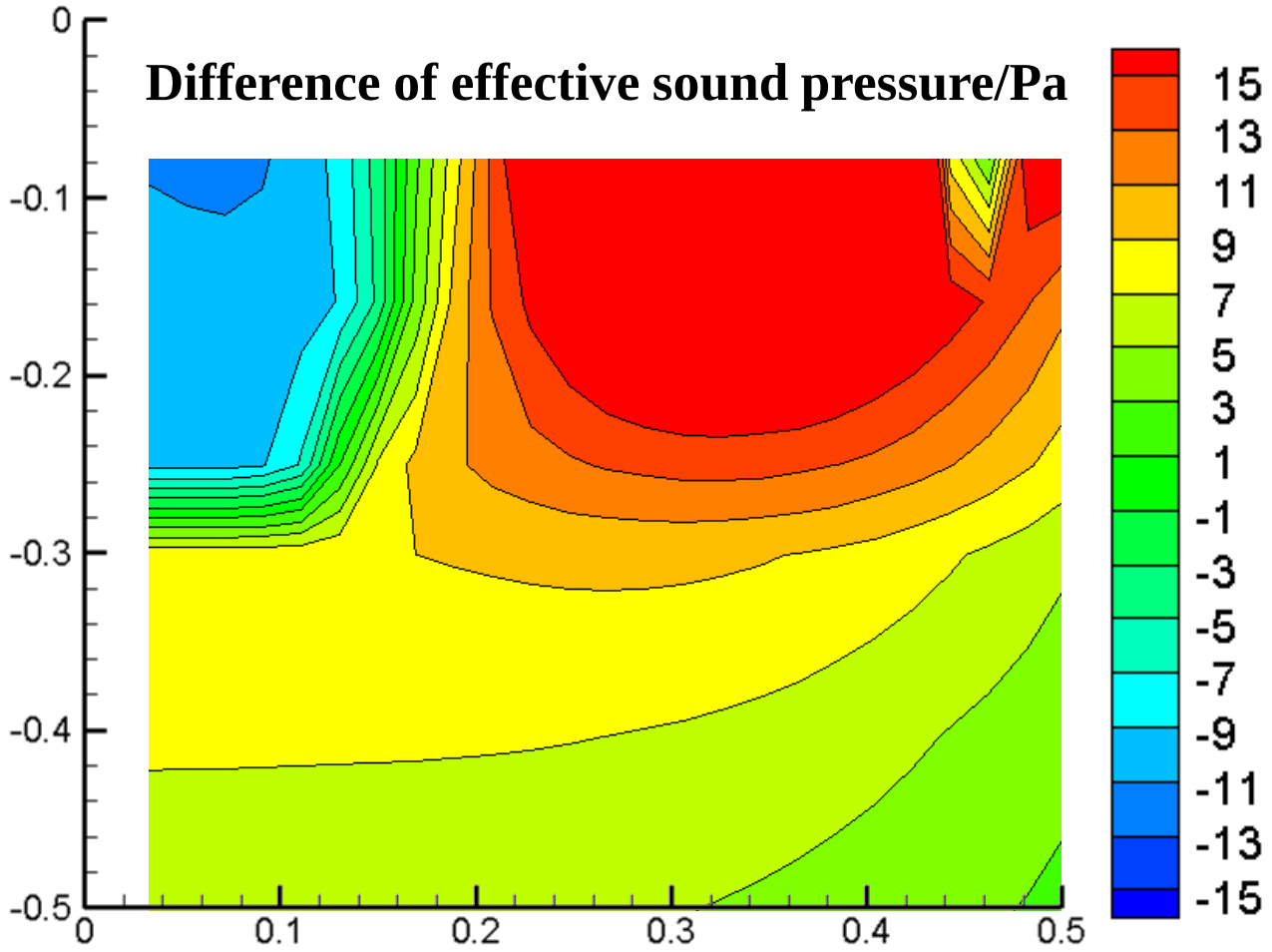

Difference of the effective sound pressure at different monitoring positions between the clean rotor, and rotor D.

This indicates that the small variation of the blade shape, at the early stage of ice accretion, can be detected by the variation of the blade acoustic characteristics.

In the yellow and green regions, the difference of effective sound pressure is too low, and the acoustic monitor cannot detect the ice. In the red regions, the effective sound pressure increases. As a result, these regions are appropriate for monitor installation. Similarly, the blue region is also a good monitoring area, although the effective sound pressure decreases there.

ACOUSTIC CHARACTERISTICS OF ICED ROTORS WITH DIFFERENT ICING POSITIONS

The ice length and ice shape of these two iced rotors are the same as rotor D, the only difference is the icing position. The icing position of rotor E is from 0.53R to 0.56R, and that of rotor F is from 0.33R to 0.36R.

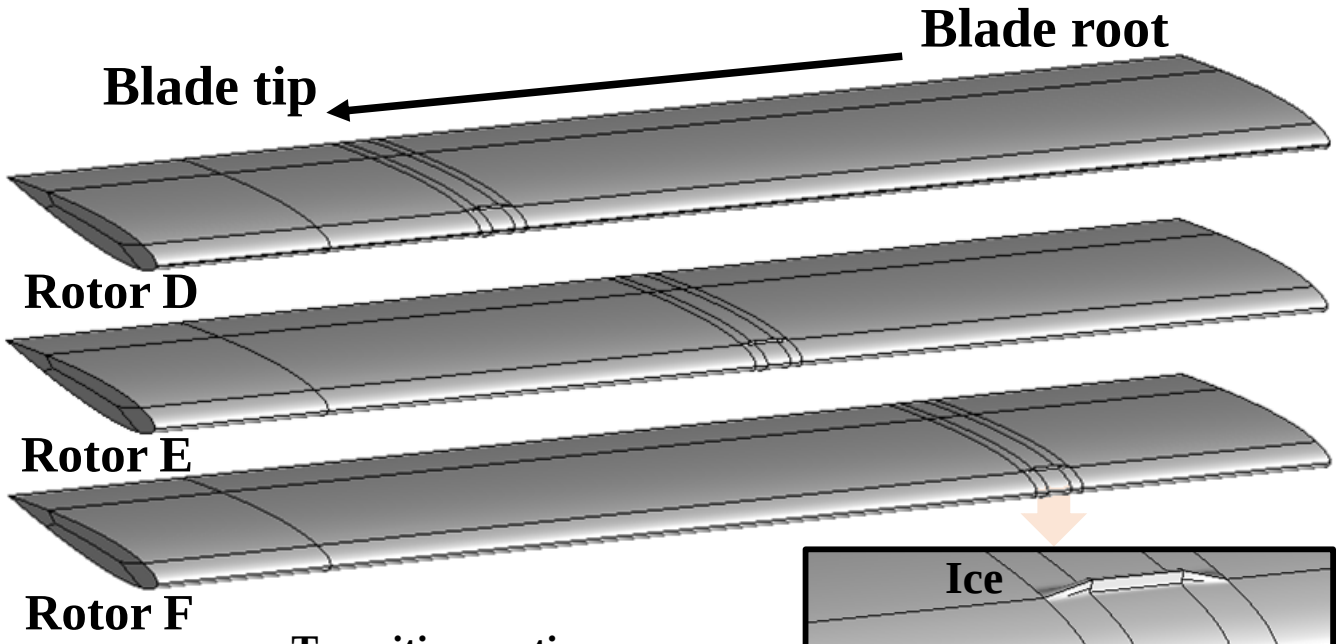

Number	D	E	F
Icing position	0.75R	0.55R	0.35R

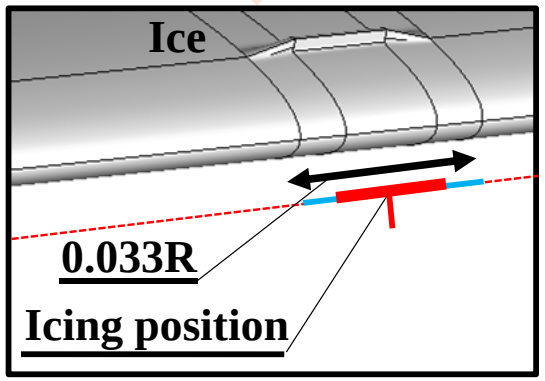

Aerodynamic performance of different iced rotors in hover

Aerodynamic characteristics	C_T	C_Q	FM	Variation of FM
Clean	1.10×10^{-2}	1.17×10^{-3}	0.492	
Rotor D	1.06×10^{-2}	1.21×10^{-3}	0.454	-7.69%
Rotor E	1.07×10^{-2}	1.20×10^{-3}	0.461	-6.31%

With ice moving to the blade root, the variation of the FM decreases.
However, the ice accretion has little effect on the aerodynamic characteristics of these three rotors.

The effective sound pressure of different iced rotors below the rotor plane in hover

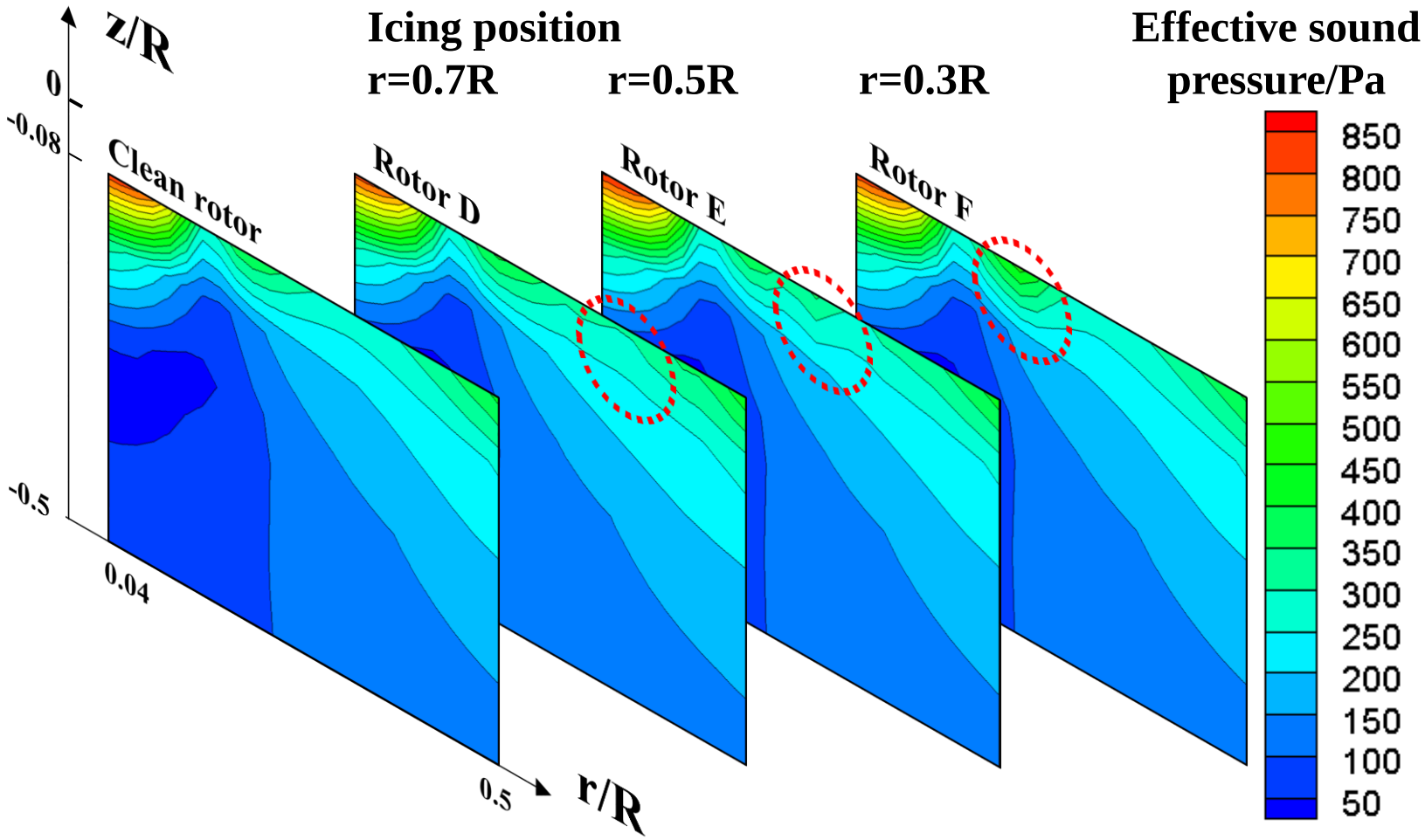

Since the ice amounts on rotors E and F are very small, the changes of the effective sound pressures in general are not appreciable.

However, the influence of the icing position on the effective local sound pressure of the rotor is clear

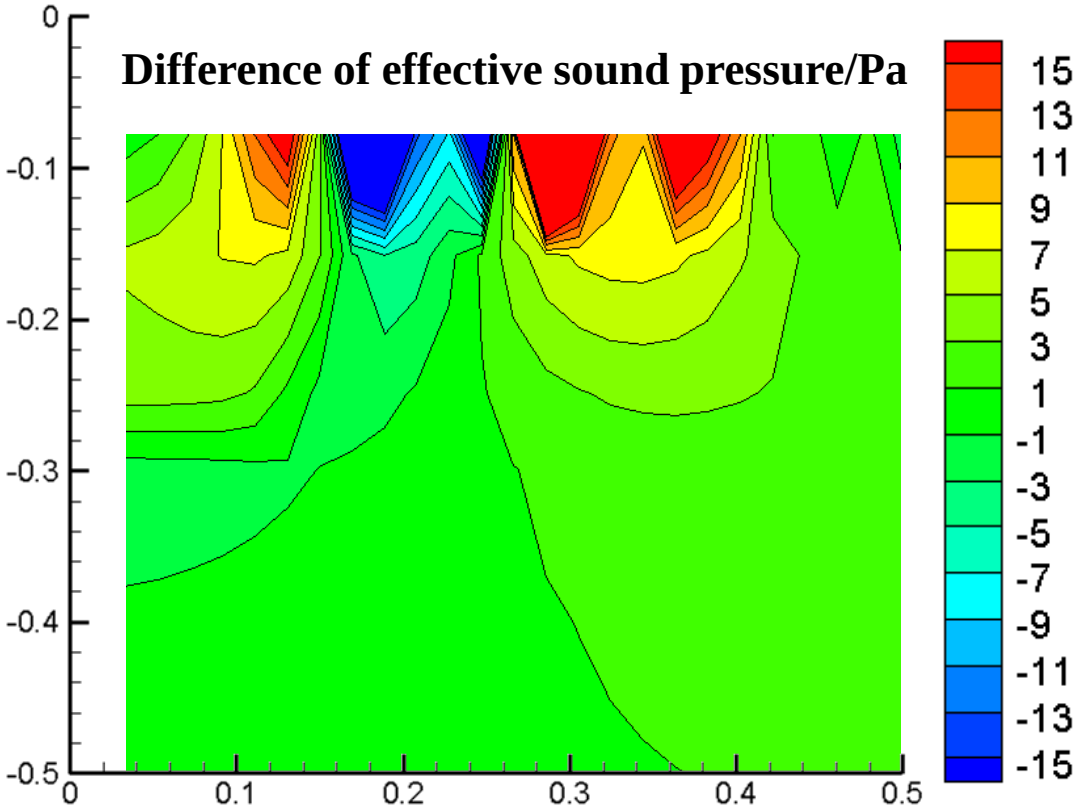

(a) Rotor E

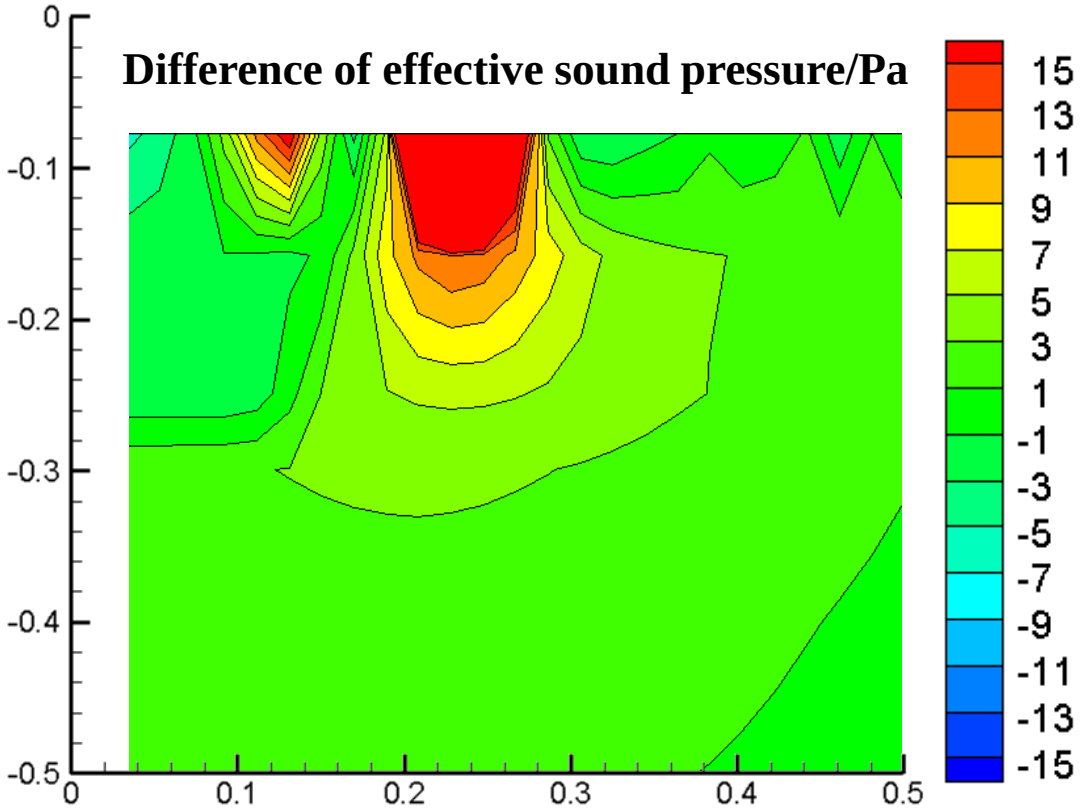

(b) Rotor F

The difference of effective sound pressure between iced rotors and clean rotor

For rotor E, the obvious variation area (differences greater than 5 or less than 5 Pa) is from r=0.1R to r=0.42R along the radial direction and near the z=-0.15 plane.

For rotor F, the obvious variation area is from r=0.1R to r=0.3R along the radial direction and near the z=-0.2 plane. Combining with rotor D above, ice can change the effective sound pressure in a limited area, and this area is from the blade root to the icing position along the radial direction.

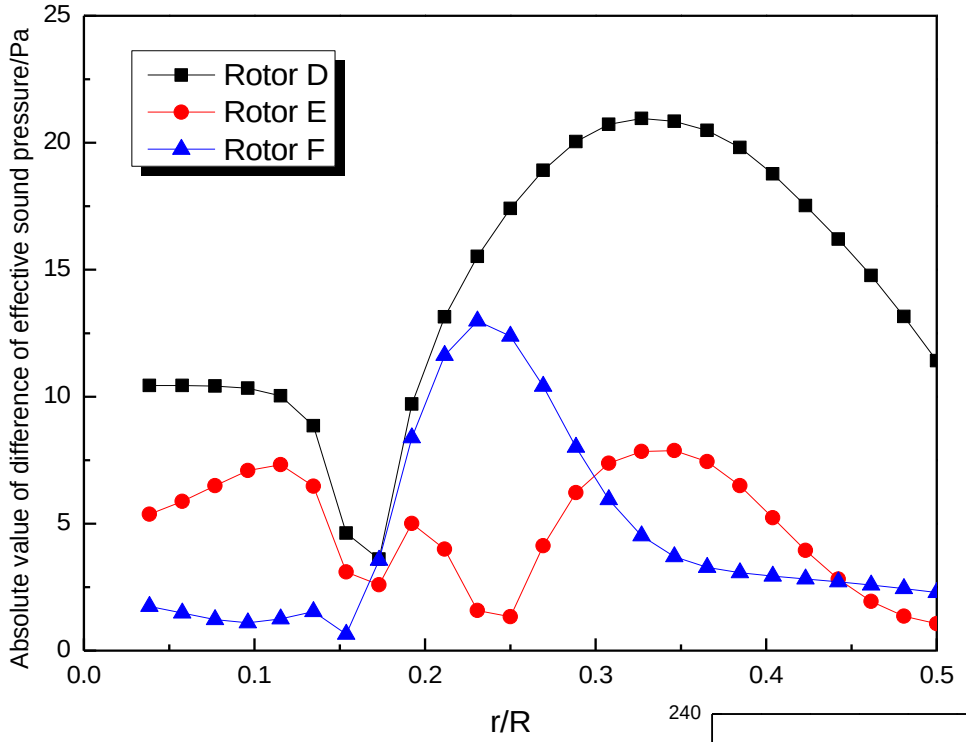

The absolute values of the differences in the effective sound pressure on the z=-0.16R plane

When the icing position is closer to the blade tip, such as for rotor D, the region of the effective sound pressure variation is larger. When the icing position is closer to the blade root, such as for rotor F, the region of the effective sound pressure variation is small.

total sound pressure time histories on the z=-0.16R plane

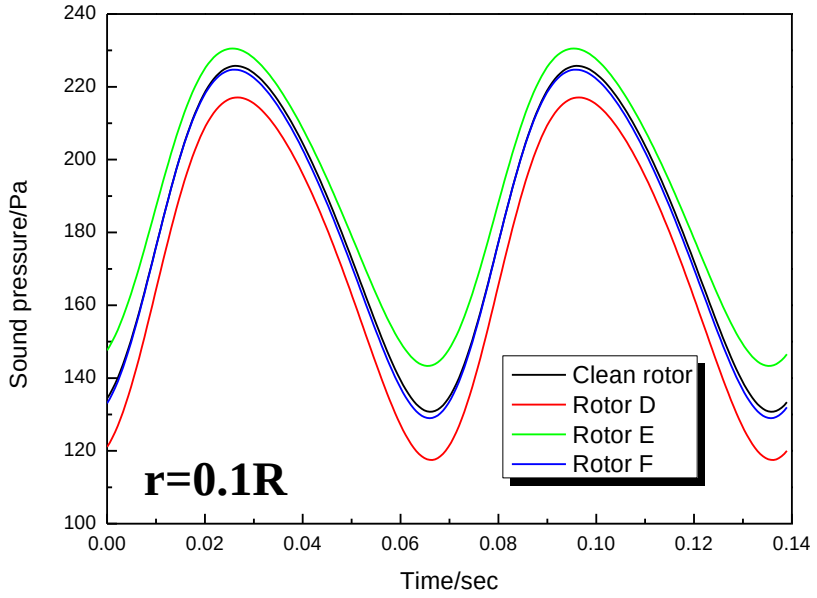

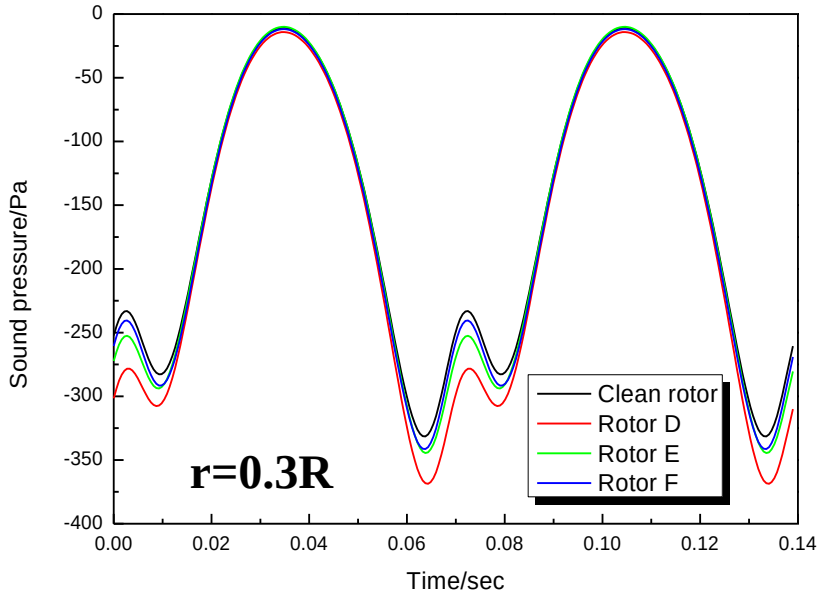

The monitor signal depends on the icing position and microphone localization, hence a microphones array needs to be used.

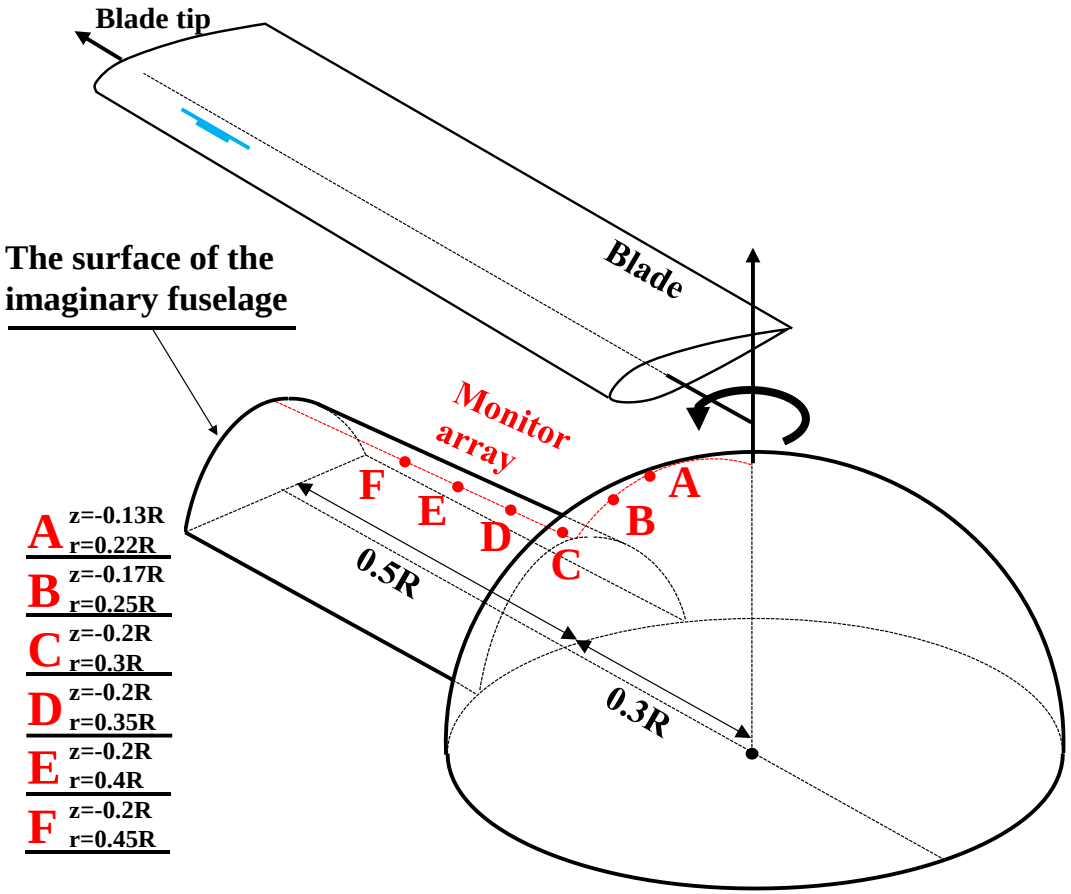

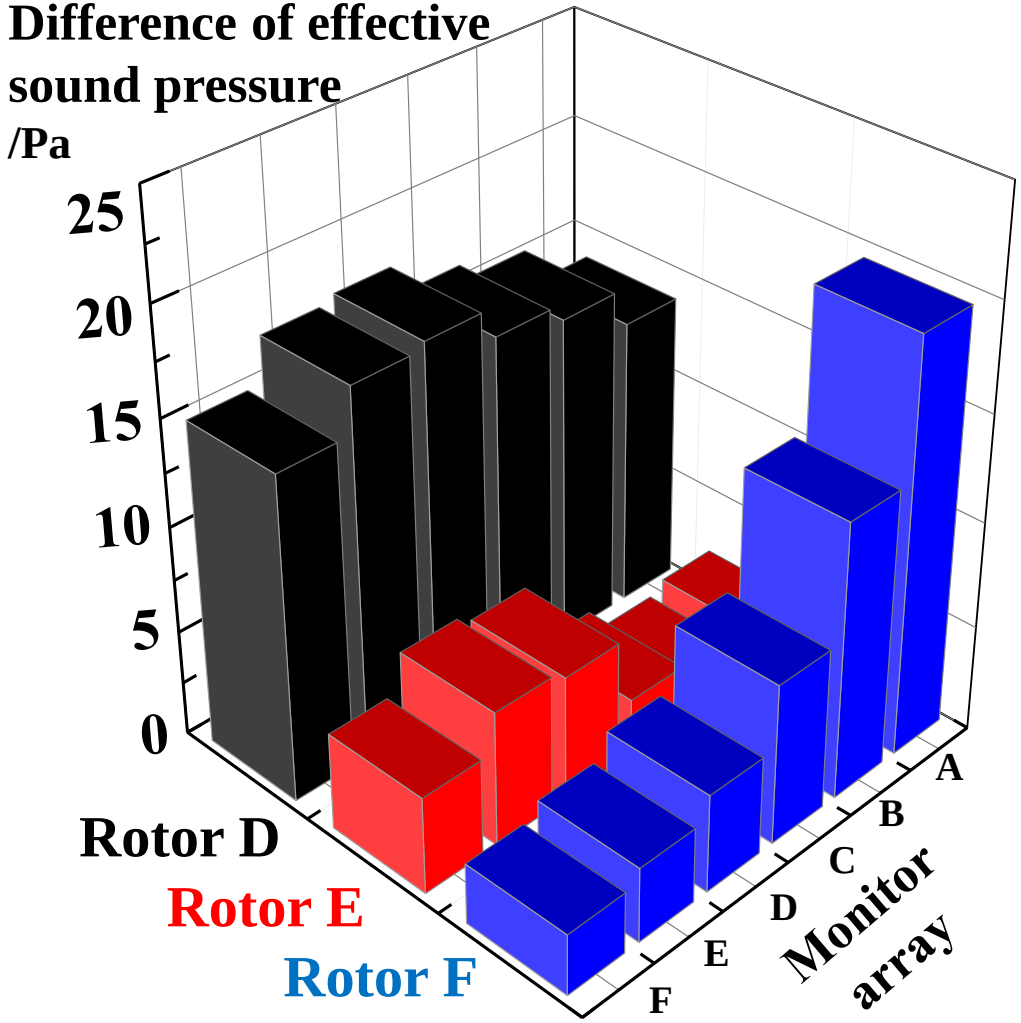

The imagery fuselage is a simple hemisphere with a radius of 0.3R and a half column with a radius of 0.125R.

The calculated result of monitor array for different iced rotors

Assumption: the monitor only can sense the value of ΔEffective sound pressure which is greater than 5 Pa.

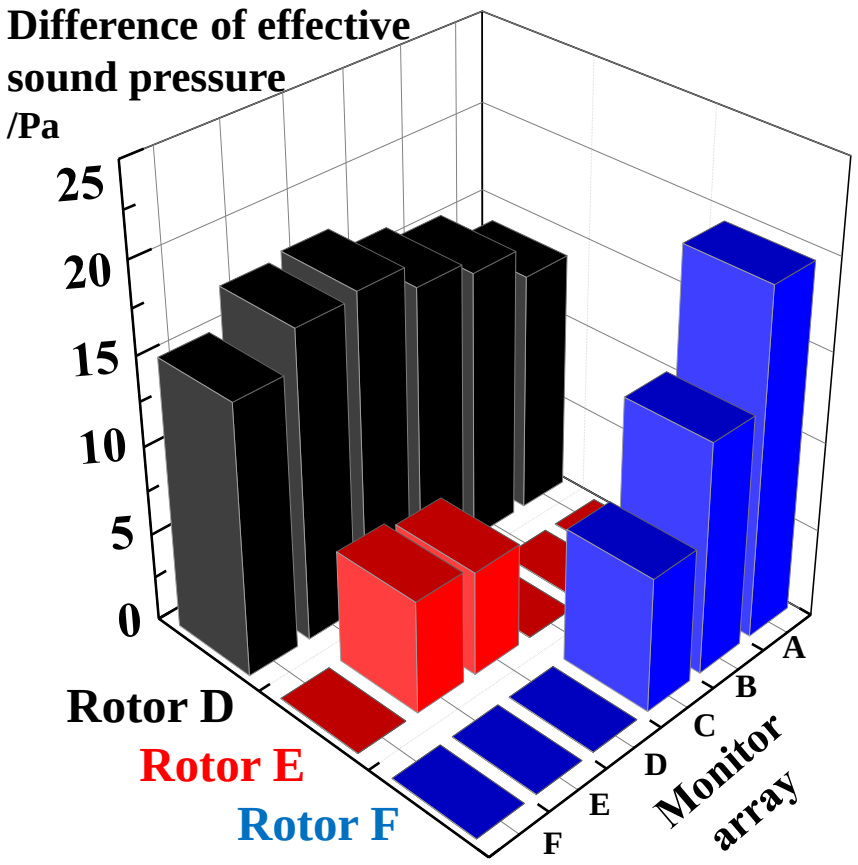

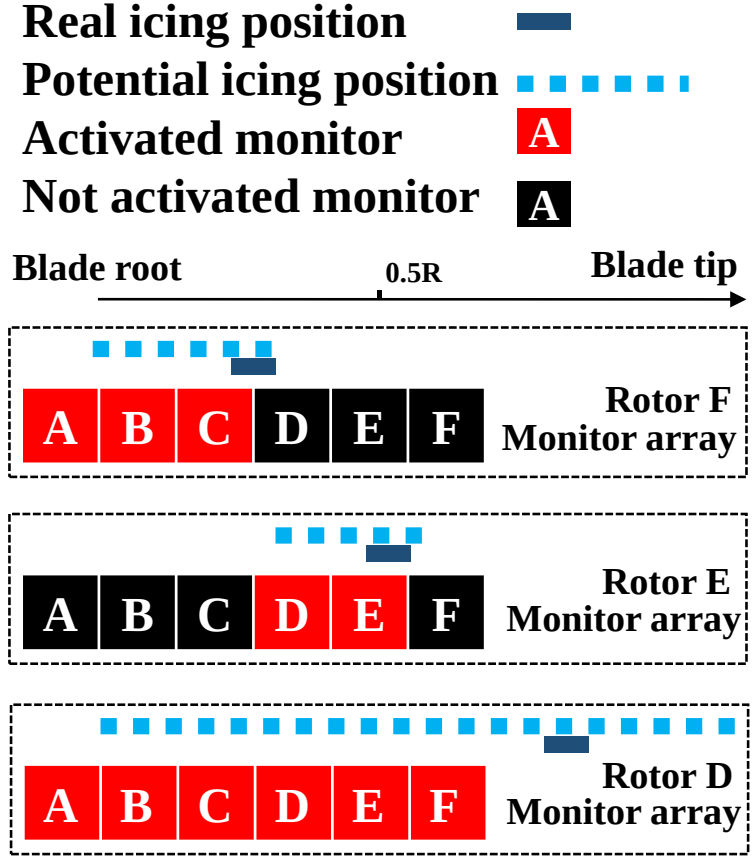

If monitors (D, E and F) are not activated, ice may not be detected on the blade from 0.3R section to the blade tip.

If monitors (A, B and C) are not activated, ice may not be detected on the blade from the blade root to 0.3R.

If monitor F is not activated, ice may not be detected on the blade from 0.5R to the blade tip.

If monitors are all activated, ice can be detected on the whole blade.

CC III: ACOUSTIC CHARACTERISTICS OF A ROTOR IN FORWARD FLIGHT WITH A SHORT ICE SHAPE

Based on the above analysis, UH-60A rotors with and without ice are computed in forward flight. The ice length is very short, and it is only 0.012R. The icing position on rotor G is from 0.594R to 0.606R, and on rotor H is from 0.694R to 0.706R.

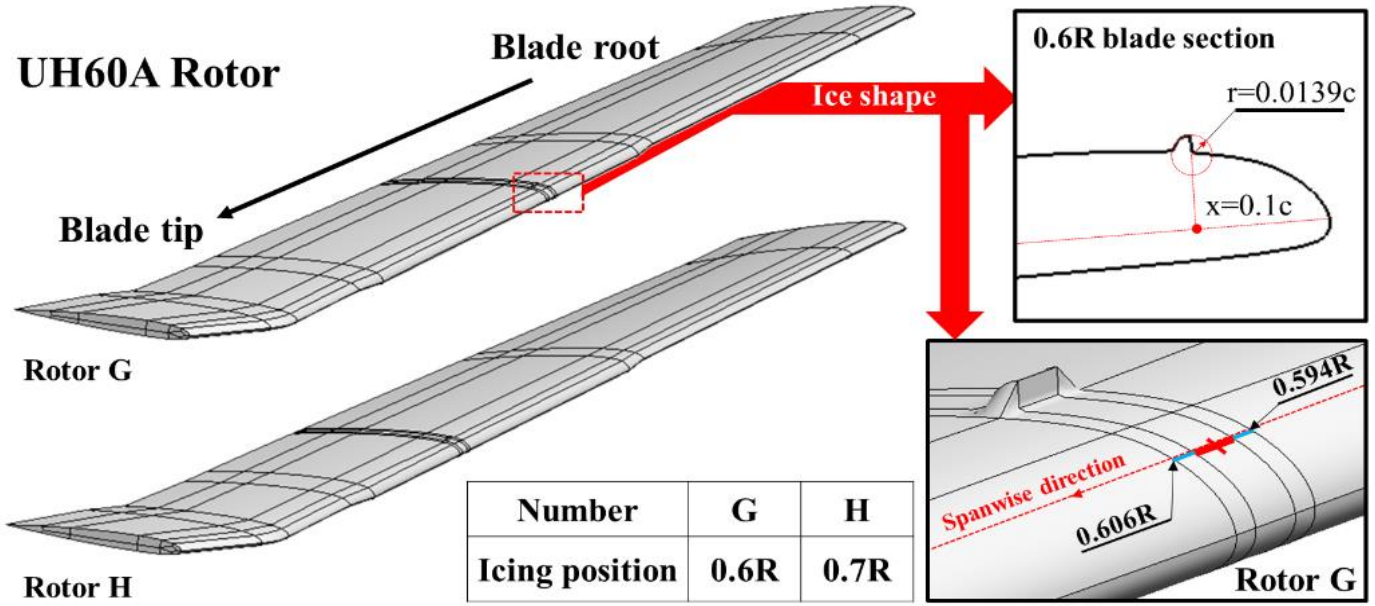

Number	G	H
Icing position	0.6R	0.7R

Icing position on the UH-60A rotor and sectional ice shape

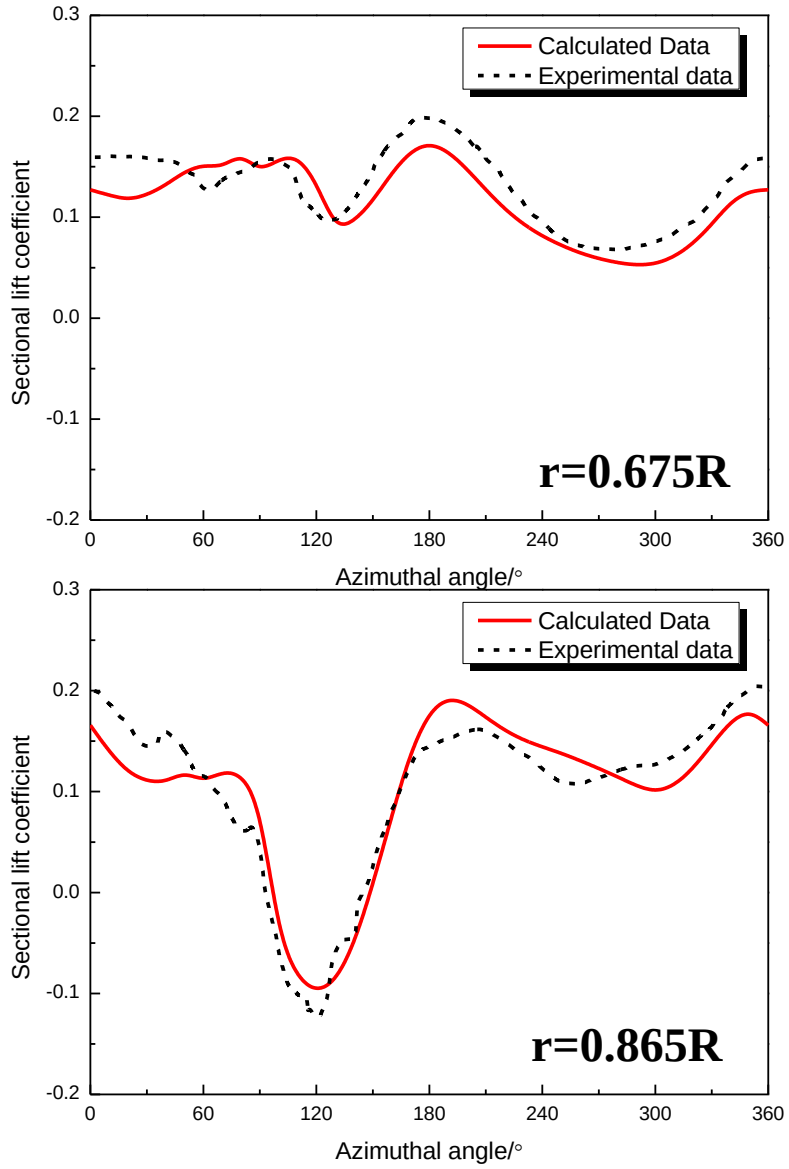

Sectional lift coefficient of the clean UH-60A rotor in forward flight

16 M cells for the rotor in FF, again with the Chimera method

Unsteady cases with 0.25 degree steps

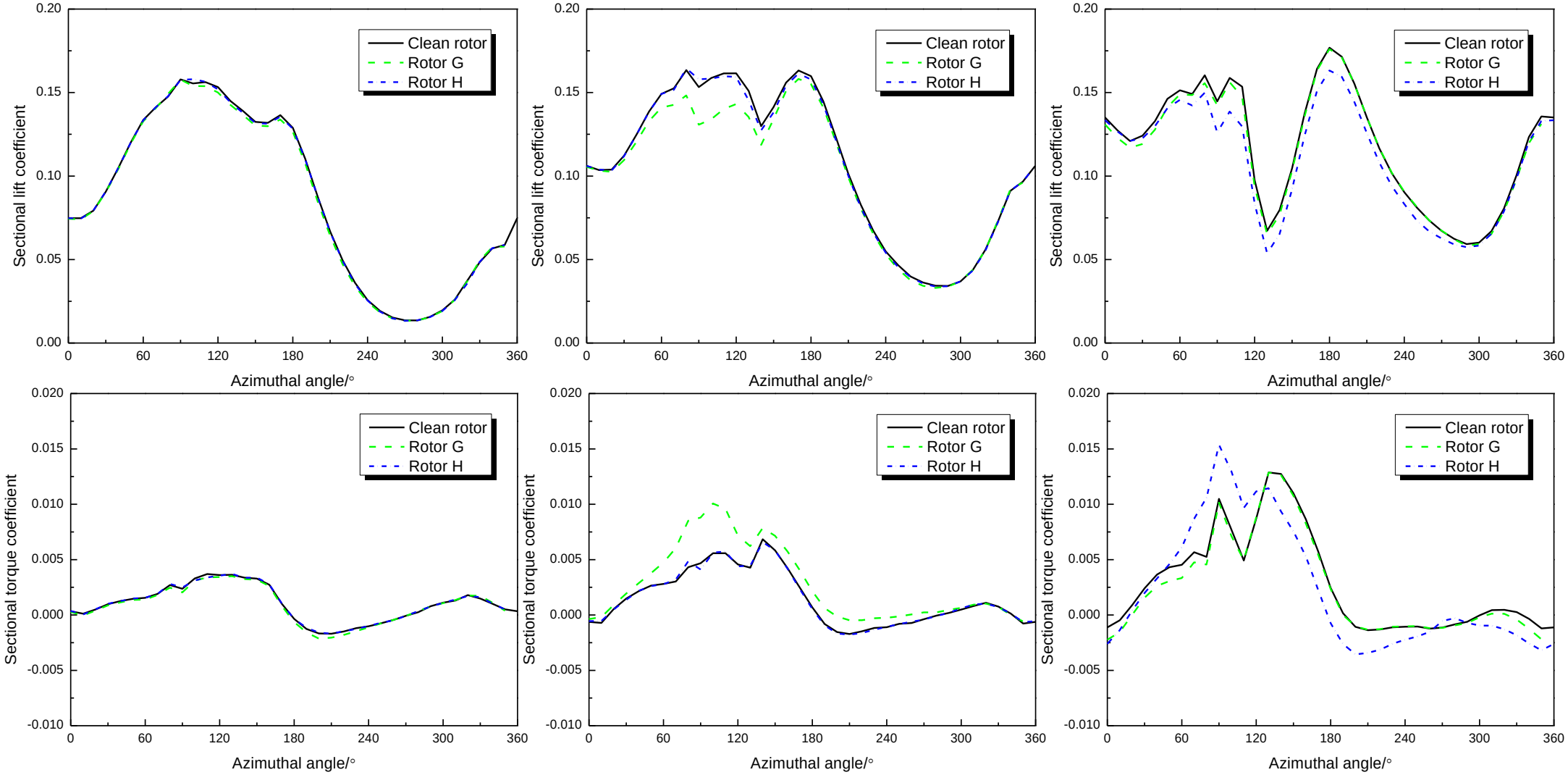

(a) r=0.5R **(b) r=0.6R** **(c) r=0.7R**

Ice is difficult to be detected by the variation of the aerodynamic characteristics.

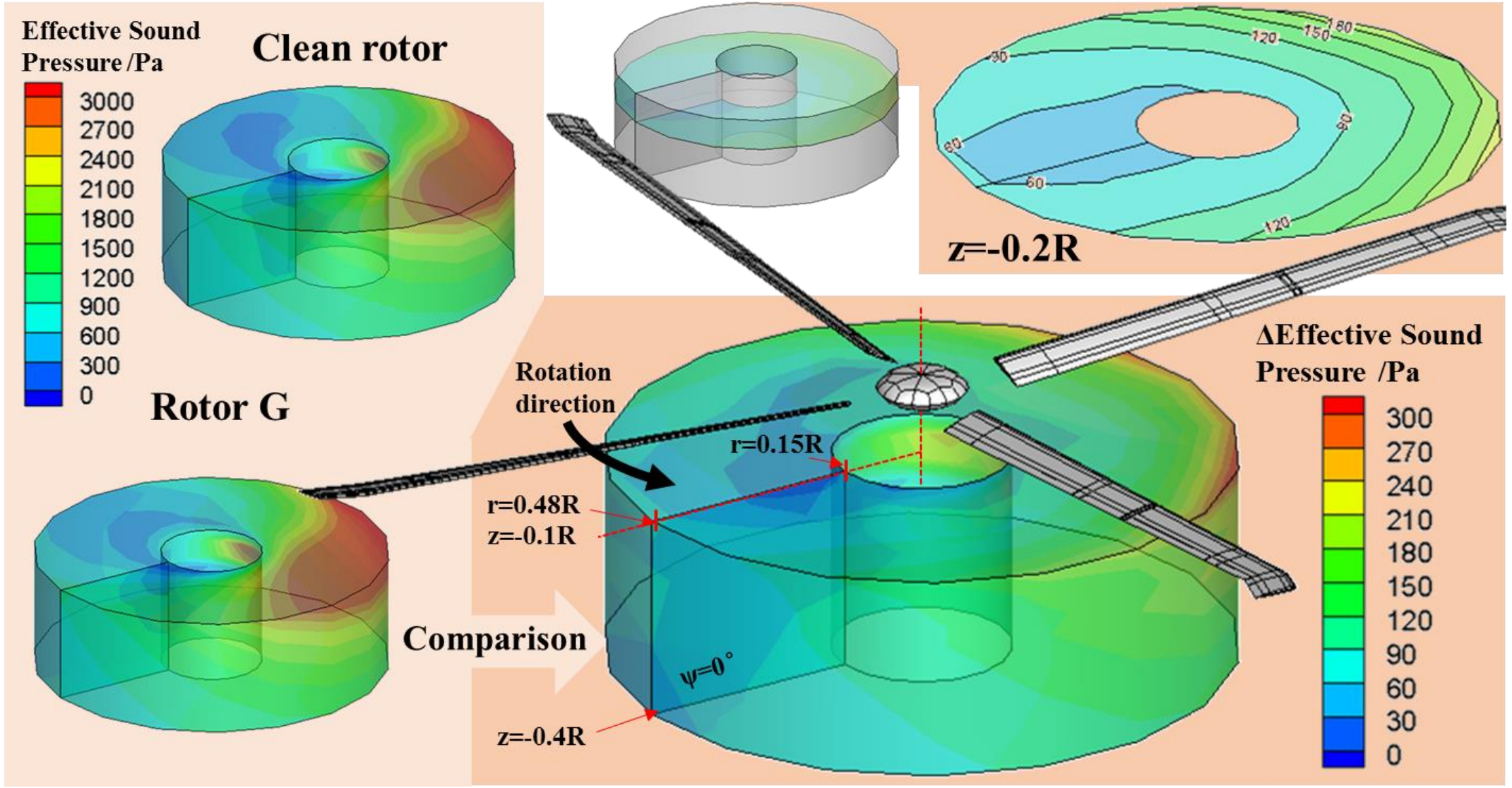

Difference of the effective sound pressure of the clean UH60A rotor and rotor G

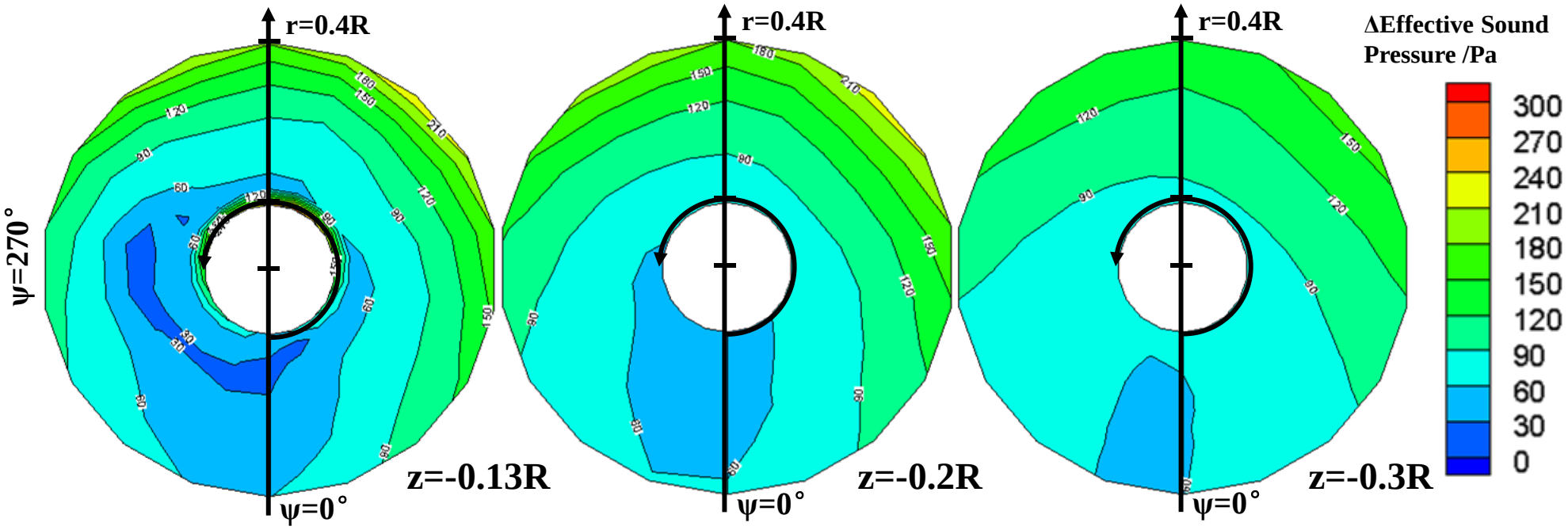

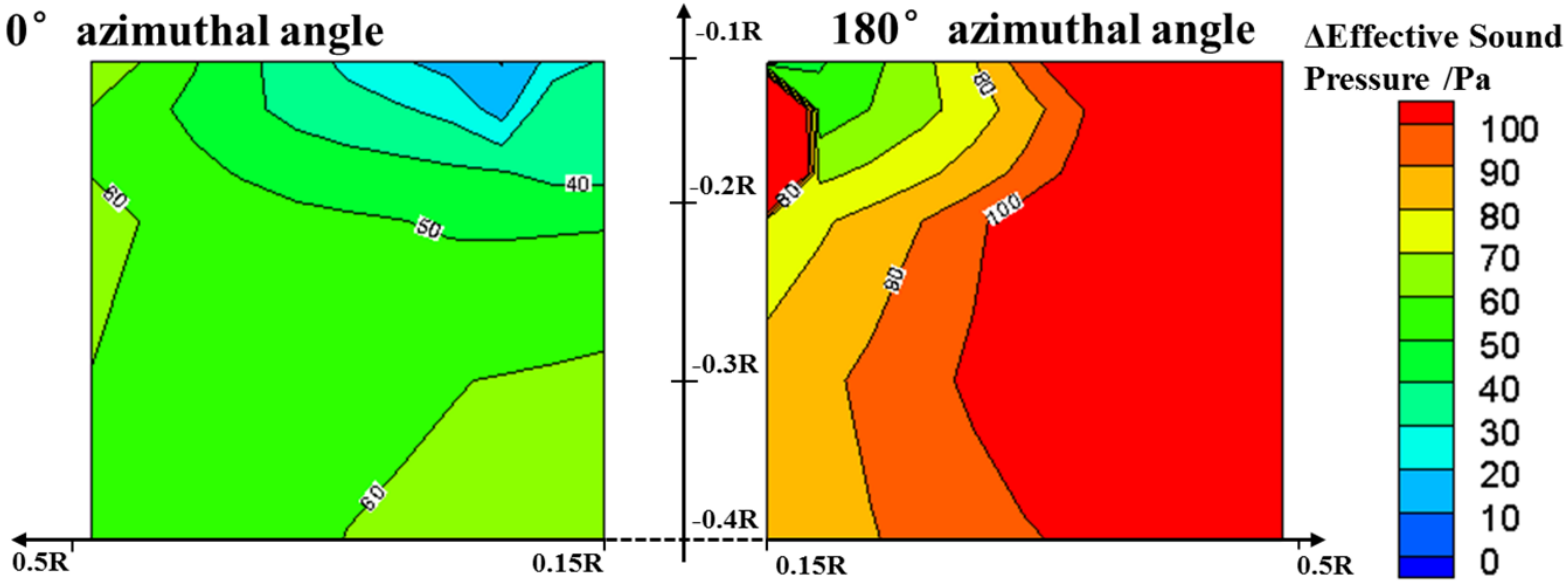

ΔEffective sound pressure is obvious enough to detect ice, and the acoustic characteristic variations are different around the azimuth, unlike hover.

ΔEffective sound pressure of rotor H is greater than the rotor G, since the icing position is different.

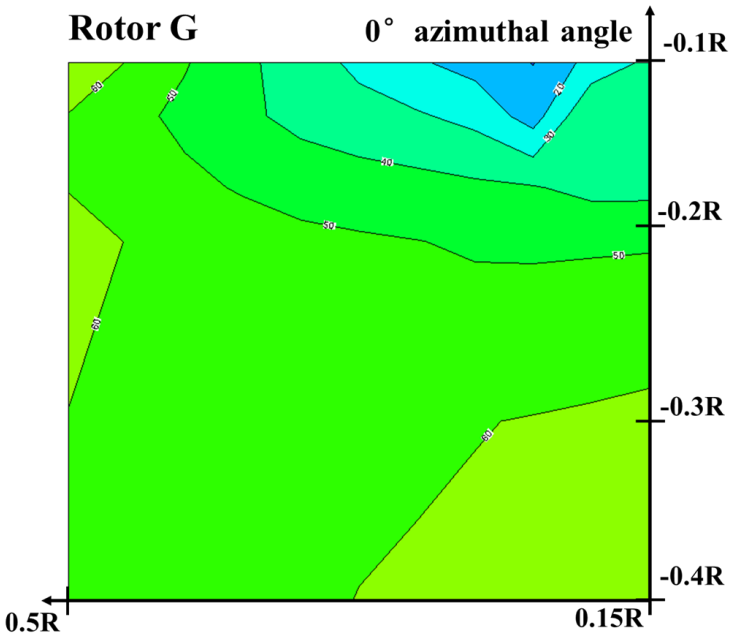

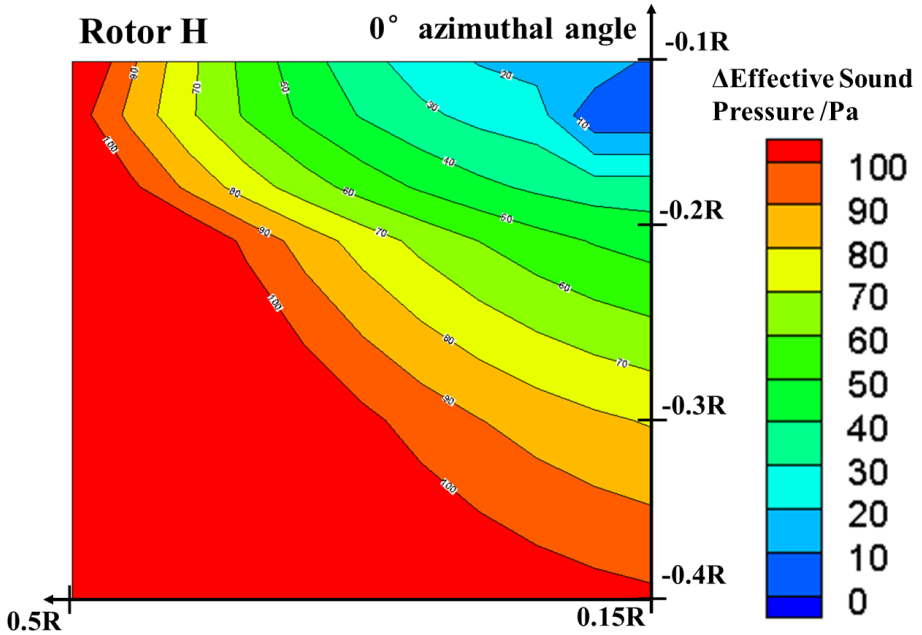

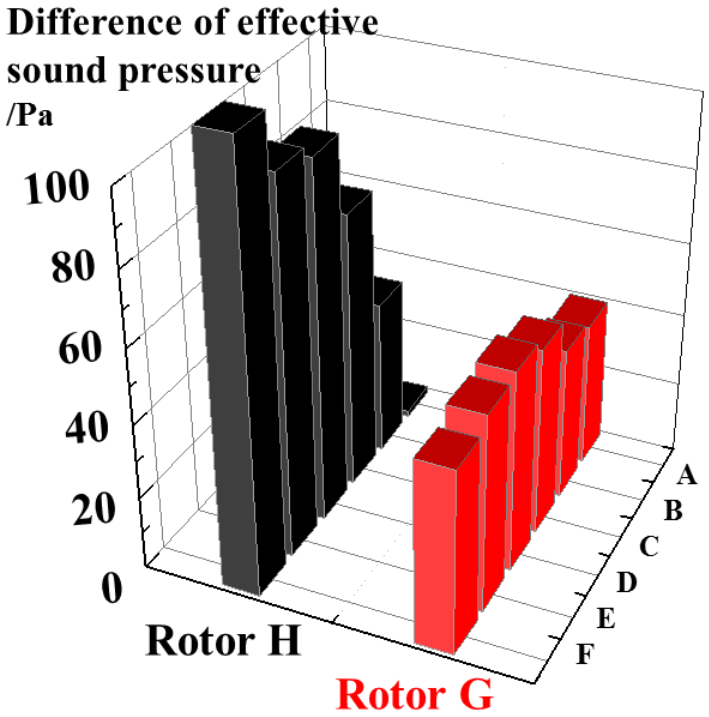

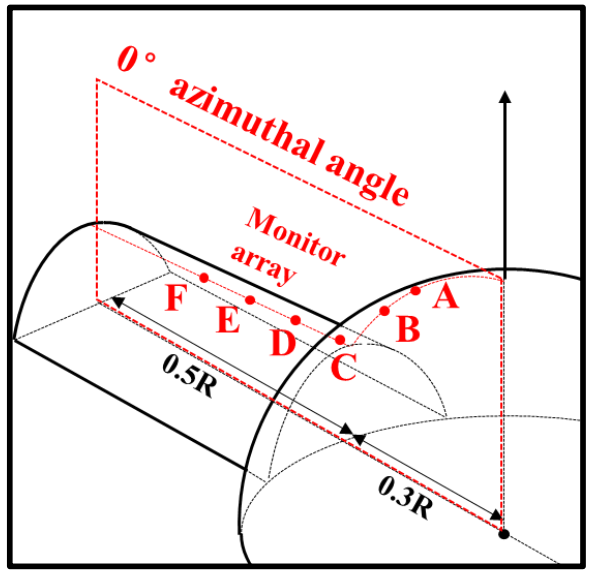

Considering the loading is greater than the hover case, the difference of the effective sound pressure is also greater. For this forward flight case, an assumption is given that the monitor only can sense the value of difference of the effective sound pressure which is greater than 50 Pa.

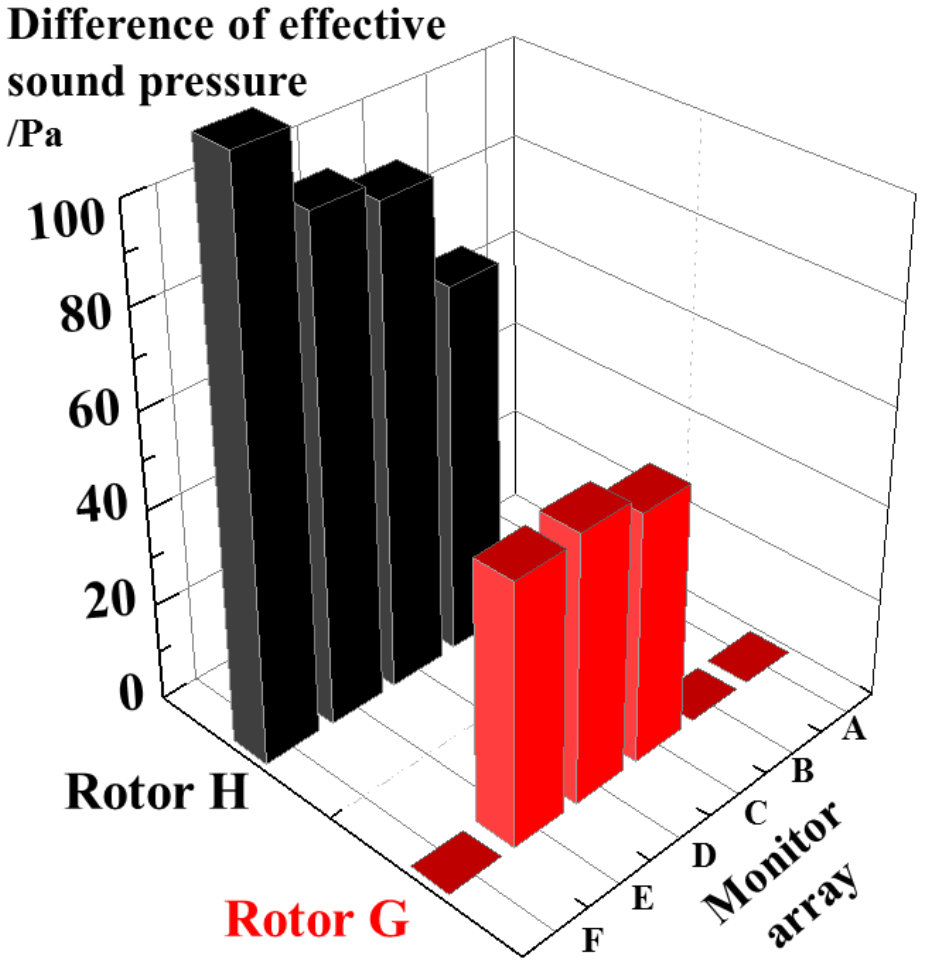

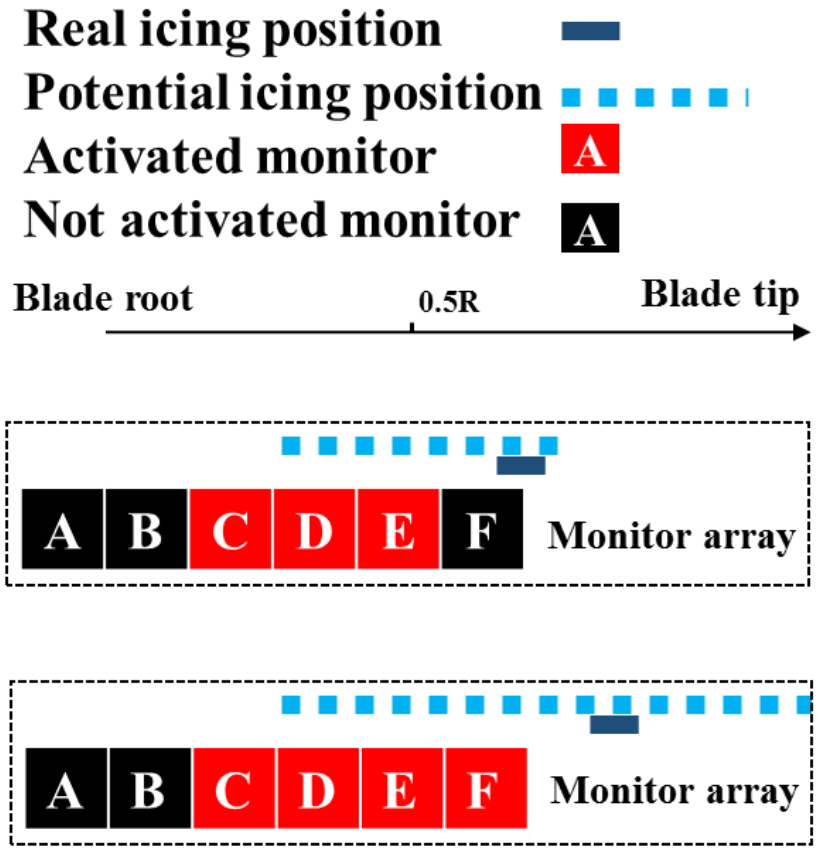

Monitors (A, B and F) are not activated, it means the ice may not occur on the blade section from the blade root to 0.3R and the section from 0.7R to blade tip.
Monitors (A, B) are not activated, it means the ice may not occur on the blade from the blade root to 0.3R section.

Obviously, the potential icing position obtained from monitor array is consistent with the real icing position of rotors G and H.

SUMMARY & CONCLUSIONS

1) Aero-acoustic characteristics of rotors are greatly influenced by ice accretion.

- **Overall, the effect of ice on the acoustics increases with the decrease of the vertical distance of the microphone, and slightly increases with the increase of the radial distance.**
- **The variation of the thickness noise will be small if the volume of ice is small.**

2) Ice on rotors can be detected at certain microphone positions near the rotor plane.

- **If the ice length is short, the sound pressure will only change in a limited region along the blade radius.**

3) If ice is formed near the blade root, the signal captured by monitors near the blade root changes, while that by monitors near the blade tip remains unchanged.

4) Through variations of the sound pressure at different monitoring points, the icing position on the rotor can be detected, especially if several monitors are used.

FUTURE STEPS OF THIS RESEACH

1) **Enhanced simulations**
   - **Perform computations with rotor and fuselage.**
   - **Enhance the resolution of the CFD computations using hybrid RANS/LES methods**
2) **Detection algorithm**
   - **Using CFD-generated signals, develop automatic detection of ice.**
   - **ANN reconstructing the SPL at the microphones ahead of the measurements**
   - **Comparison of measured and ANN signals, and decision logic development**

THANK YOU!